Predominant floodplain over mountain weathering of Himalayan sediments (Ganga basin)

Maarten LUPKER[1*], Christian FRANCE-LANORD[1], Valier GALY[2], Jérôme LAVÉ[1], Jérôme GAILLARDET[3], Ananta Prasad GAJUREL[4], Caroline GUILMETTE[1], Mustafizur RAHMAN[5], Sunil Kumar SINGH[6], Rajiv SINHA[7]

[1]Centre de Recherches Pétrographiques et Géochimiques (CRPG-CNRS), 15 rue Notre Dame des Pauvres, 54501 Vandoeuvre les Nancy, France.

[2]Woods Hole Oceanographic Institution (WHOI) - Department of Marine Chemistry and Geochemistry, 266 Woods Hole Rd., Woods Hole, MA 02543, USA.

[3]Institut de Physique du Globe (IPGP), 1 rue Jussieu, 75238 Paris, France.

[4]Department of Geology, Tri-Chandra Campus, Tribhuvan University, Kathmandu, Nepal.

[5]Department of Soil Science, University of Dhaka, Bangladesh.

[6]Physical Research Laboratory (PRL), Navrangpura, Ahmedabad, 380009, India.

[7]Engineering Geosciences Group, Indian Institute of Technology (IIT), Kanpur, 208016, India.

*Corresponding author: mlupker@crpg.cnrs-nancy.fr

1 **Abstract**

2 We present an extensive river sediment dataset covering the Ganga basin from the Himalayan

3 front downstream to the Ganga mainstream in Bangladesh. These sediments were mainly

4 collected over several monsoon seasons and include depth profiles of suspended particles in

5 the river water column. Mineral sorting is the first order control on the chemical composition

6 of river sediments. Taking into account this variability we show that sediments become

7 significantly depleted in mobile elements during their transit through the floodplain. By

8 comparing sediments sampled at the Himalayan front with sediments from the Ganga

9 mainstream in Bangladesh it is possible to budget weathering in the floodplain. Assuming a

10 steady state weathering regime in the floodplain, the weathering of Himalayan sediments in

11 the Gangetic floodplain releases ca. $(189 \pm 92) \cdot 10^{9}$ and $(69 \pm 22) \cdot 10^{9}$ moles/yr of carbonate

12 bound Ca and Mg to the dissolved load, respectively. Silicate weathering releases $(53 \pm$

13 $18) \cdot 10^{9}$ and $(42 \pm 13) \cdot 10^{9}$ moles/yr of Na and K while the release of silicate Mg and Ca is

14 substantially lower, between ca. 0 and $20 \cdot 10^{9}$ moles/yr. Additionally, we show that sediment

15 hydration, $[H_2O^+]$, is a sensitive tracer of silicate weathering that can be used in continental

16 detrital environments, such as the Ganga basin. Both $[H_2O^+]$ content and the D/H isotopic

17 composition of sediments increases during floodplain transfer in response to mineral

18 hydrolysis and neoformations associated to weathering reactions. By comparing the chemical

19 composition of river sediments across the floodplain with the composition of the eroded

20 Himalayan source rocks, we suggest that the floodplain is the dominant location of silicate

21 weathering for Na, K and $[H_2O^+]$. Overall this work emphasizes the role of the Gangetic

22 floodplain in weathering Himalayan sediments. It also demonstrates how detrital sediments

23 can be used as weathering tracers if mineralogical and chemical sorting effects are properly

24 taken into account.

25

1. INTRODUCTION

Chemical weathering is central in surface biogeochemical cycles because it redistributes the chemical elements between Earth's surface reservoirs such as continental crust and the Ocean. Over geological timescales, silicate weathering coupled with carbonate precipitation in the Ocean is responsible for a large fraction of atmospheric sequestration that balances the mantle and metamorphic CO_2 inputs into the atmosphere and therefore regulates the global climate (e.g. Walker et al., 1981; Berner et al., 1983). These considerations have fostered research from small-scale mineral dissolution studies (e.g. Oelkers and Schott, 1995; White and Brantley, 2003) to global scale weathering models (e.g., Berner, 1994; Donnadieu et al., 2004). While modern weathering rates are often derived from river solute fluxes (e.g. Meybeck, 1987; Gaillardet et al., 1999a; West et al., 2005), their solid counterparts have received far less attention (e.g. Gaillardet et al., 1999b; France-Lanord and Derry, 1997; Gislason et al., 2006) probably because of the difficulty of integrating the variability of detrital sediments over space and time (Lupker et al., 2011; Bouchez et al., 2011a; 2011b; 2011c). Sediment records are however one of the rare archives that can be reliably used to trace past erosion fluxes at regional scales.

In an effort to understand and quantify the link between the chemical composition of river sediments and chemical weathering, we present a study of modern sediments within the Ganga fluvial network. Silicate weathering within the Himalayan system – the largest active orogen and highest mountain range on Earth - has retained much attention (e.g. Raymo et al., 1988; Derry and France-Lanord, 1996; Galy and France-Lanord, 1999) as it is commonly assumed that chemical weathering is directly associated with physical erosion, triggered by relief and elevation. However, the spatial budget and *locus* of weathering within the

3

51 Himalayan system has never been properly determined, even though a predominant role of the

52 floodplain compartment in the weathering budget of the Himalayan system has been proposed

53 (Galy and France-Lanord, 1999; West et al., 2002). The Ganga River system is draining the

54 central-western part of the Himalayan orogen where high erosion rates are responsible for

55 large sediment load (c.a. 400-500 Mt/yr for the Ganga in Bangladesh, RSP, 1996; Lupker et

56 al., 2011) that transit through an extensive floodplain before being discharged to the Indian

57 Ocean. Heretofore, the role of this extensive floodplain in the chemical weathering process

58 has remained poorly constrained.

59

60   We characterize the weathering signature of river sediments collected in the

61 floodplain, along a transect from the Himalayan front downstream to the outflow of the

62 Ganga in Bangladesh and further compare these sediments to the Himalayan source rocks. We

63 use mobile to immobile ratios of major elements, carbonate content and hydration of

64 sediments (hereafter referred to as $[H_2O^+]$) to trace and quantify chemical weathering.

65 Sediment hydration marks the uptake of protons by hydrolysis or neo-formation of hydroxyl-

66 rich secondary minerals and can therefore be used as weathering tracer. Additionally, the

67 hydrogen stable isotopic composition (D/H) of the hydroxyl groups reflects the isotopic

68 composition of the water from which they were formed (Savin and Epstein, 1970; Lawrence

69 and Taylor, 1971, 1972; Gilg and Sheppard, 1996) and can potentially be used as a tracer for

70 the weathering locus.

71

72   **2. STUDY SETTING**

73

74   **2.1. Hydrological and erosional setting**

75

51 Himalayan system has never been properly determined, even though a predominant role of the

52 floodplain compartment in the weathering budget of the Himalayan system has been proposed

53 (Galy and France-Lanord, 1999; West et al., 2002). The Ganga River system is draining the

54 central-western part of the Himalayan orogen where high erosion rates are responsible for

55 large sediment load (c.a. 400-500 Mt/yr for the Ganga in Bangladesh, RSP, 1996; Lupker et

56 al., 2011) that transit through an extensive floodplain before being discharged to the Indian

57 Ocean. Heretofore, the role of this extensive floodplain in the chemical weathering process

58 has remained poorly constrained.

59

60   We characterize the weathering signature of river sediments collected in the

61 floodplain, along a transect from the Himalayan front downstream to the outflow of the

62 Ganga in Bangladesh and further compare these sediments to the Himalayan source rocks. We

63 use mobile to immobile ratios of major elements, carbonate content and hydration of

64 sediments (hereafter referred to as $[H_2O^+]$) to trace and quantify chemical weathering.

65 Sediment hydration marks the uptake of protons by hydrolysis or neo-formation of hydroxyl-

66 rich secondary minerals and can therefore be used as weathering tracer. Additionally, the

67 hydrogen stable isotopic composition (D/H) of the hydroxyl groups reflects the isotopic

68 composition of the water from which they were formed (Savin and Epstein, 1970; Lawrence

69 and Taylor, 1971, 1972; Gilg and Sheppard, 1996) and can potentially be used as a tracer for

70 the weathering locus.

71

72   **2. STUDY SETTING**

73

74   **2.1. Hydrological and erosional setting**

75

76   The Ganga River system is mainly fed by tributaries draining the Himalayan range.

77   From west to east, the Yamuna, the Ganga, the Karnali, the Narayani and the Kosi are all

78   major rivers draining the Himalayan range with basin size ranging from 7600 km^2 for the

79   Yamuna to 57800 km^2 for the Kosi. The three main Nepalese Himalayan Rivers (Karnali,

80   Narayani and Kosi) join the Ganga mainstream after a long transit (200 to 600 km) in the

81   Indogangetic floodplain, where the Karnali and Narayani are respectively renamed Ghaghara

82   and Gandak. The westernmost Himalayan tributaries of the Ganga, the Yamuna drains

83   through the city of Delhi and merges with the Ganga in Allahabad, ca. 900 km downstream of

84   the Himalayan front (Figure 1).

85   Non Himalayan Rivers also contribute to the sediment and dissolved load of the Ganga, in

86   particular southern tributaries. The Chambal River – the largest southern tributary of the

87   Ganga (Rengarajan et al., 2009) – is draining the front of the Vindhya Range and part of the

88   Deccan traps and joins the Yamuna River in the Gangetic plain (Figure 1). After a total transit

89   in the floodplain of ca. 1500 km the Ganga merges with the Brahmaputra, which drains the

90   eastern part of the Himalaya and the southern border of the Tibetan plateau. The confluence

91   of the Ganga and Brahmaputra in Bangladesh forms the Lower Meghna that delivers the

92   products of Himalayan erosion to the Bay of Bengal and the Indian Ocean. The total drainage

93   area of the Ganga covers 1.06 million km^2 of which 17% lies in the Himalaya, 35% in the

94   Indian shield and 48% in the Ganga plain (Rao, 1979).

95   The major part of the 380 km^3 Ganga's yearly discharge (WARPO hydrological data)

96   occurs during the monsoon season from June to September (Fasullo and Webster, 2003), and

97   approximately 54 % of this discharge is derived from the Himalayan catchments, 22% from

98   the southern tributaries and the remaining 24 % from the floodplain itself (Rao, 1975; Singh

99   et al., 2008). The sediment flux exported by the Ganga is estimated at ca. 400 to 500 Mt/yr of

100   which 90 to 95 % is transported during the monsoon (RSP, 1996; Lupker et al., 2011). Less

101 than 10% of the eroded Himalayan flux is stored in the Gangetic floodplain (Lupker et al.,

102 2011).

103

104   **2.2. Geological setting**

105

106   The Himalayan crust is commonly divided in four main east-west striking geological

107 units. From north to south: the Tethyan Sedimentary Series (TSS), the High Himalaya

108 Crystalines (HHC), the Lesser Himalaya (LH) and the Siwaliks. These units are bound by

109 major faults: the South Tibetan Detachment (STD) between the TSS and HHC; the Main

110 Central Thrust (MCT) between the HHC and LH; the Main Boundary Thrust (MBT) between

111 the LH and Siwaliks and the Main Frontal Thrust (MFT) at the southern front of the range.

112 The TSS are composed of weakly metamorphosed, carbonate rich, late Cambrian to Eocene

113 marine sedimentary sequences. The HHC are formed by Neoproterozoic to Ordovician high

114 grade metamorphic rocks, marbles and local intrusions of leucogranite. The LH are low-grade

115 mostly sedimentary rocks composed of quartzites, phyllites, black shists to limestones, or

116 orthogneiss. To the south, the Siwalik consists of Neogene floodplain deposits uplifted by the

117 southern propagation of the deformation front. Thanks to contrasted signatures of HHC and

118 LH units in Sr and Nd isotopic compositions, Galy and France-Lanord (2001) estimated that

119 80% of the sediments eroded from the Himalayas are derived from the HHC, and the

120 remaining 20% of the LH, even though river incision (Lavé and Avouac, 2001) or lithology of

121 transported pebble (Attal and Lavé, 2006) show that TSS and Siwalik sediments may also

122 represent a significant part of the eroded material in central Nepal.

123   Further south, the Himalayan front is bound by the 200 to 300 km wide Ganga.

124 foreland basin. Below the Ganga alluvial plain, several kilometers of sediments eroded from

125 the Himalayan range overlay the Archean to Early Proterozoic Indian craton (Lyon-Caen and

126 Molnar, 1983).

127 In the southern part of the basin, the Chambal River drains very different lithologies

128 compared to Himalayan Rivers. The Chambal headwaters and its tributaries are draining the

129 Cretaceous tholeiitic lava flows of the Deccan Traps that cover a significant part of the

130 drainage area and Neoproterozoic to Paleoproterozoic marine deposits mainly composed of

131 sandstones and limestone (Rengarajan et al., 2009 and references therein).

132

133 **3. SAMPLING STRATEGIES AND ANALYTICAL PROCEDURES**

134

135 **3.1. River sediment sampling**

136

137 Rivers in the Ganga basin were repeatedly sampled mainly during the monsoon

138 season, in 2001, 2002, 2004, 2007, 2008, 2009 and 2010. All major tributaries of the Ganga in

139 Nepal, India and Bangladesh were sampled over these 7 years of field campaigns. When

140 possible, sediments were sampled along vertical depth profiles to document the chemical

141 heterogeneity and derive accurate average chemical compositions of the transported material.

142 The main trans-Himalayan tributaries of the Ganga, from east to west: the Yamuna, the

143 Ganga, the Karnali, the Narayani and the Kosi River were sampled at the front of the

144 Himalayan range near the MFT. Additionally, samples from the Eastern and Central

145 watersheds of the Karnali River (Bheri and upper Karnali) near the MBT (upstream of the

146 MFT) were included in this study. The trans-Himalayan Rivers (Ganga, Karnali, Narayani

147 and Kosi) were sampled further downstream in the floodplain, before their confluence with

148 the mainstream Ganga or another major river (except for the Yamuna that was sampled after

149 its confluence with the Chambal). The contribution of Siwalik sediments to the sediment load

150 was characterized using samples from the Rapti River - a tributary of the Karnali draining

151 mainly Siwalik units - and from more minor tributaries such as the Suraï, Tinau and Rapti

152 Chitwan. The Chambal River, the main river draining the southern part of the Ganga basin,

153 was sampled upstream its confluence with the Yamuna. The Gomti River, disconnected from

154 any direct Himalayan input (Singh et al., 2005) was used as an analogue for pure floodplain

155 sediment input in the Ganga basin. The Ganga mainstream was also sampled in Varanasi

156 (Benares) and Patna in the floodplain. Finally, the Ganga mainstream was repeatedly sampled

157 during the monsoon season (2002, 2004, 2007, 2008 and 2010) at Harding Bridge

158 (Bangladesh). This station located before the confluence of the Ganga with the Brahmaputra

159 integrates all major tributaries contributions to the Ganga River load (Figure 1).

160   Sampling included: (1) suspended sediment depth profiles in the water column that

161 allow to capture the full sedimentological variability, (2) dredged bedload samples and (3)

162 recent flood deposits or bank sediments. The detail of sampling techniques and preparation

163 can be found in (Galy et al., 2008; Lupker et al., 2011). Part of the sampling presented in this

164 work have already been used to document organic carbon fluxes (Galy et al., 2007; 2008),

165 residence and transfer times in the Ganga basin (Granet et al., 2007; 2010), mineralogical

166 variability (Garzanti et al., 2010; 2011) and to budget global sediment fluxes and composition

167 (Lupker et al., 2011).

168

169   **3.2. Sample analysis**

170

171   Major elements, carbonate content and sediment hydration where determined to

172 characterize the weathering signature of exported river sediments.

173

174 *3.2.1. Major elements*

175

176   Sediments were first powdered in an agate mortar. Major element concentrations were

177   measured by ICP-AES and ICP-MS at "Service d'Analyse des Roches et des Minéraux"

178   (SARM – CRPG, Nancy-France) on bulk aliquots of ~ 100 mg of sediment after lithium

179   metaborate fusion (Govindaraju and Mevelle, 1987; Carignan et al., 2001). The relative

180   uncertainty for major elemental concentration is better than 2%.

181

182   *3.2.2. Carbonate content determination*

183

184   Carbonates contents were manometricaly determined from the CO_2 released after

185   reaction with H_3PO_4 with 30 to 50 mg sample on a manual vacuum extraction line. Calcite

186   was determined after 3 hr at 25°C, and dolomite content was sequentially determined after

187   additional 7 days reaction at 50°C (Sheppard and Schwarcz, 1970; Galy et al., 1999). The

188   isotopic compositions of calcite and dolomite where measured on the released CO_2 by a

189   modified VG-602 mass spectrometer and are reported using $\delta^{18}O$ (SMOW) and $\delta^{13}C$ (PDB)

190   notations. The reported reproducibility is ± 0.1 ‰.

191

192   *3.2.3. Hydration and D/H stable isotopic composition in sediments*

193

194   Existing methods for D/H analysis in rocks (Sharp et al., 2001; Gehre and Strauch,

195   2003; Gong et al., 2007; Garzione et al., 2008) were adapted to analyze detrital, clay rich

196   sediments and to ensure a high sample throughput. Between 2 to 8 mg of powdered sample

197   were analyzed on-line using an Elemental Analyzer (EA) coupled to a VG Isoprime Isotope

198   Ratio Mass Spectrometer (IRMS). Details of the analytical procedure are given bellow.

199   First, adsorbed and inter-layer water needs to be removed. No general consensus on

200   the elimination procedure of adsorbed water can be found in the literature. Proposed

201   procedures have explored heating the sample to 250°C under vacuum for 2 to 3 hours (Savin

202   and Epstein, 1970), 200°C for 12 hours (Girard et al., 2000), 350°C for 4 hours (Gong et al.,

203   2007) or 70°C under vacuum for 20 days (Garzione et al., 2008). Yapp and Pedley (1985) and

204   Girard et al. (2000) also used up to 3 hours pumping at 100°C to remove exchangeable water

205   from natural goethites. In our procedure, samples were pre-weighted in tin capsules, placed in

206   a sample carrousel and degassed at 120°C under vacuum for 48h in a degassing canister.

207   Great care was taken to use constant degassing temperature and time for all samples to ensure

208   internal reproducibility of the data. Degassing for less than 48h resulted in higher variability

209   in sample water content and isotopic composition that was attributed to remaining adsorbed

210   water. After dehydration, the degassing canister was placed in a dry, N_2 flushed, glovebox. In

211   the glovebox, the sample carrousel was transferred in a custom, sealed, automatic sampler

212   pre-flushed with He. This automatic sampler was then reconnected to the EA and evacuated

213   for c.a. 20 min before opening it to the reduction column. This procedure suppresses any

214   contact of samples with atmospheric moisture that could rapidly re-hydrate the samples and

215   was found to increase overall reproducibility of the $[H_2O^+]$ and D/H measurements.

216   Samples were combusted on an EA glassy carbon reaction tube, packed with glassy

217   carbon chips and enclosed in a ceramic liner to reduce hydroxyls to H_2. The temperature of

218   the column was kept at 1450°C by a Kanthal-Superthal heating element. High temperature

219   was required to ensure rapid sample reduction, to prevent CH_3 formation (Burgoyne and

220   Hayes, 1998) and to improve the reproducibility as already noticed by other authors (Sharp et

221   al., 2001; Gehre and Strauch, 2003). He carrier pressure was maintained at 120 kPa and the

222   produced gases were separated on a chromatographic column kept at 60°C. After

223   chromatographic separation, H_2 was introduced in the MS source through an open-split and

224   analyzed for D/H isotopic composition. H^{3+} correction was performed for each sample from

225 in house H_2 standard injections covering the sample signal range. The source trap current was

226 kept at 500 mA and the samples were measured with a major peak height between 6 and 10

227 nA. The amount of H_2 produced was determined by comparing the major peak area with the

228 signal produced during the analysis of internal standards.

229   Three different internal standards (Muscovite: MuscD65, Phlogopite: Mica-Mg and a

230 fine grained marine sediment from the bay of Bengal: SO188) were routinely included during

231 sample analysis to account for instrumental drift. These internal standards were calibrated

232 against IAEA reference material NBS30 (Biotite, δD = -65.7 ‰), NBS22 (Oil, δD = -120 ‰)

233 and CH-7 (Polyethylene, δD = -100.3 ‰) for D/H isotopic composition and MS linearity.

234 $[H_2O^+]$ of the internal standards were calibrated against analysis of the same internal

235 standards degassed using the same procedure on a classical extraction line involving

236 extraction of water and subsequent reduction on a uranium furnace (Biegelsen et al., 1952).

237 D/H is reported as δD and is normalized against SMOW. The overall, long term, 1 σ,

238 reproducibility of the method on sediments and rocks is generally better than 2 ‰ for δD

239 similar to the reproducibility obtained by Sharp et al., (2001) or Garzione et al., (2008) and

240 0.1 % for $[H_2O^+]$ (Figure A1, Appendix A). Samples were analyzed as duplicates.

241

242   **4. RESULTS**

243

244   The detailed composition of sediments used in this work is reported in the

245 supplementary data file, table S1.

246

247   **4.1 Mineral sorting and weathering systematic**

248

249   The vertical depth profiles retrieved from rivers of the Ganga basin show a strong

250   heterogeneity of the chemical composition of suspended sediments within the water column

251   (Figure 2). Heterogeneities in river sediment chemistry as a function of sampling depth have

252   been previously described for the Ganga-Brahmaputra and other large river (e.g. Galy et al.,

253   2007; Bouchez et al., 2011a; 2011b; Garzanti et al., 2011; Lupker et al., 2011). The

254   hydrodynamic control on the chemical composition of sediments in the Ganga River has been

255   detailed in Lupker et al., 2011 and linked to mineral sorting effects (Garzanti et al., 2011).

256   Briefly, the river hydrodynamical conditions of the sampled water column control the

257   suspension of sediments based on their grain size, shape and density. For poly-mineralogical

258   sediments, this results in a mineralogical and thus chemical differentiation of sediments

259   within the water column.

260   The dominant minerals controlling the distribution of major elements in the water

261   column are summarized in Table 1. Ganga sediment mineralogy is dominated by quartz, mica

262   and feldspar, with occurrence of other phylosilicates, clay assemblages and hydroxides in the

263   finer fraction. Calcite and dolomite are also abundant. For detailed mineralogical analysis see

264   Garzanti et al. (2010) and Garzanti et al. (2011). In the Ganga River basin, sediment load

265   increases bottomward by a factor of 2 to 3 between the shallowest and deepest samples. As

266   illustrated in Figure 2, the major element composition of suspended sediments is variable

267   from surface to bottom. SiO_2 concentration increases bottomward from 50 - 60 wt% in

268   surface samples to 60 - 75 wt% for the deepest suspended sediments and up to 85 wt% in

269   bedload samples. Na_2O concentrations in surface sediments also generally increase from

270   surface (ca. 0.9 wt%) to bottom (ca. 1.1 to 1.3 wt%) for Himalaya front Rivers while Ganga

271   sediments in Bangladesh have typical concentrations between ca. 1.0 and 1.2 wt%. On the

272   contrary, Al_2O_3, Fe_2O_3, K_2O and H_2O^+ show decreasing concentrations bottomward. Al_2O_3

273   concentrations range from ca. 15 - 18 wt% in surface samples to ca. 10 - 14 wt% for the

274   deepest samples and down to 7 - 8 wt% in bedload samples. Fe_2O_3 concentrations range from

275   6 - 8 wt% in surface samples to 4 to 6 wt% in the deepest samples down to 2 - 3 wt% in the

276   bedload. K_2O concentrations of typical surface sediments are of the order of 3 - 4 wt% and

277   decrease to 2 - 3 wt% in deep sediments and 1 - 2 wt% in bedload samples. H_2O^+

278   concentrations range from ca. 3 - 4 wt% in surface samples to 1 - 2 wt% in deeper samples

279   and down to 0.5 wt% in bedload samples. The D/H isotopic composition of sediments ranges

280   from - 70 to - 110 ‰ and is not clearly dependant on sampling depth. Dolomite and calcite

281   content of sediments is also highly variable depending on tributaries (from 0 to over 20 wt%)

282   and shows no clear dependence with depth. As CaO and MgO contents reflect both carbonate

283   and silicate detrital sources, the concentrations of CaO and MgO show a poor dependence

284   with depth.

285

286   The large variability of sediment composition found in a single water column has to be

287   accounted for to derive reliable information on the downstream evolution of the sediments

288   during their transfer in the Gangetic floodplain. Following Galy and France-Lanord (2001)

289   and in order to disentangle mineralogical sorting signals from the true chemical downstream

290   evolution of sediments in large rivers, major elements were first normalized to silicon content

291   to exclude dilution effects. Various elemental ratios of sediments are then evaluated with

292   respect to their Al/Si molar ratio. Al/Si is used as a proxy of mineral sorting effects and is

293   strongly correlated to grain size (Lupker et al., 2011). Coarse-grained sediments are enriched

294   in quartz and have thus a low Al/Si ratio while finer grained surface sediments tend to be

295   enriched in phylosilicates and clay minerals that have higher Al/Si ratios. The water column is

296   thus well described by a range of Al/Si ratios and hydrodynamic mineral sorting results in a

297   binary mixing trend between two end-members characterized respectively by a low Al/Si

298   (coarse grained) and a high Al/Si (fine grained) ratio (Figure 3a). In the Himalayan system,

299   dissolved Si and Al represents only respectively ca. 1 % and less than 0.1 % of the particulate

300   flux (Galy and France-Lanord, 2001). These elements can therefore be treated, to a first

301   approximation, as immobile. Chemical weathering therefore results in the loss of the most

302   mobile elements such as Na, K, Mg, Ca or a gain in hydration at constant Al/Si for steady

303   state weathering. Hence, when considering samples collected along depth profiles, weathering

304   is marked by a decrease (increase for H_2O^+/Si) in the slope of the linear relationship between

305   mobile elements normalized to Si and Al/Si (Figure 3a). The chemical composition of the

306   exported sediment flux may further influenced by sediment sequestration in the floodplain.

307   Floodplain deposits tend to be enriched in coarse-grained and quartz-rich fractions.

308   Conversely, the remaining transported load gets enriched in finer, clay rich sediments. This

309   sequestration results in an apparent increase of the average Al/Si ratio of the transported

310   sediments during floodplain transfer (Figure 3b). For the Ganga floodplain this effect remains

311   however limited as only ca. 10 % of the transported load is deposited in the floodplain thereby

312   increasing the average Al/Si ratio of the transported load from 0.22 at the Himalayan front to

313   0.23 for the Ganga in Bangladesh (Lupker et al., 2011). The weathering of Himalayan

314   sediments can therefore be estimated by comparing the average chemical composition of river

315   sediments sampled at different locations in the floodplain.

316

317   **4.2. Spatial and temporal variation in chemical composition**

318

319   *4.2.1. Major elements*

320

321   In this work we mainly focus on variability of the Fe/Si (Figure 4), Na/Si (Figure 5),

322   K/Si (Figure 6), H_2O^+/Si (Figure 7) with respect to Al/Si ratio. All elements, but Na, show a

323   systematic positive correlation with Al/Si showing the enrichment of the finer fraction (high

324 Al/Si) in Fe, K and H_2O^+ with respect to Si and the predominance of quartz in the coarser

325 fraction (lower Al/Si ratio) as stated earlier. These correlations are linear for Fe, K and H_2O^+

326 suggesting a simple binary mixing between the coarse and fine-grained end-member. For Na

327 the relationship is more complex and suggests a mixing between more than 2 end-members.

328 These different end-members may be induced by mineralogical sorting of different minerals

329 bearing Na such as albite (Garzanti et al., 2010; 2011) or due to the heterogeneity in the

330 composition of the eroded lithologies (c.f. section 5.1.1). When considering each river

331 individually, this relationship can be reasonably approximated by a log relationship for

332 intermediate Al/Si ratios (0.15 – 0.30). The overall variability amongst rivers is higher for the

333 finer fraction than for the coarse fraction. Bed-load sediments show a uniform average

334 composition across the Gangetic plain even if some variability is observed. This second order

335 variability can be mainly attributed to placer effects and accessory minerals. For each

336 sampling year and location, the chemical composition of the sediments shows a unique

337 mixing trend between an invariant bedload end-member and a variable fine-grained end-

338 member. We will further describe the variability amongst rivers and sampling dates based on

339 these correlations.

340   The major trans-Himalayan Rivers (the Yamuna, Ganga, Karnali, Narayani and Kosi)

341 sampled at the Himalayan front (Himalayan front Rivers in Figure 4, 5, 6 and 7) show a

342 comparable Fe/Si (Figure 4.a) and K/Si (Figure 6.a.) relationship with Al/Si. The Na/Si

343 (Figure 5.a) and H_2O^+/Si (Figure 7.a) composition of these rivers shows more variability with

344 a quasi-identical composition for the Yamuna, Ganga, Narayani and Kosi but a significant

345 depletion in Na and enrichment in H_2O^+ for the Karnali sediments compared to the other

346 trans-Himalayan Rivers.

347   After transiting in the floodplain and before merging with the Ganga mainstream the

348 sediments from Himalayan Rivers (Himalayan floodplain Rivers in Figure 4, 5, 6 and 7) are

349 marked by a small but significant increase in Fe/Si ratios. Furthermore, these sediments also

350 lose Na and K while they gain H_2O^+ during their course in the Gangetic floodplain. The

351 relative loss is higher for Na than for K. Sediments from the Ganga shows the largest loss of

352 Na and gain of H_2O^+ relative to Si during floodplain transfer while sediments from the

353 Karnali and Kosi Rivers display the smallest loss/gain.

354   The sediments from the Ganga in Bangladesh, after mixing of all tributaries feeding

355 the mainstream, have on average slightly higher Fe/Si ratios than Himalayan sediments and

356 are significantly depleted in Na, K and enriched in H_2O^+ compared to Himalayan tributaries.

357 The chemical composition of sediments sampled during 6 different sampling years on the

358 Ganga in Bangladesh reveal an inter-annual variability for all elements (Figure 4c, 5c, 6c, 7c).

359 This variability was not detected for Himalayan front Rivers when two different sampling

360 years were available. The variability in sediment composition of the Ganga shows that years

361 with high Fe/Si ratios (e.g. 2005) are also marked by low Na/Si and K/Si ratio, suggesting a

362 common origin for the observed variations.

363

364   In order to derive a purely Himalayan weathering budget from the river sediments

365 across the floodplain it is necessary to correct for additional non Himalayan tributaries such as

366 the main southern tributary, the Chambal. Sediments from the Chambal have a distinct

367 chemical composition characterized by higher Fe/Si and H_2O^+/Si ratios along with lower

368 Na/Si and K/Si ratios compared to other rivers in the basin. This Chambal "fingerprint" can

369 be followed further downstream in the Yamuna after its confluence with the Chambal (in

370 Kalpi, see Figure 1) where sediments have similar chemical characteristics as Chambal

371 sediments and even in the Ganga in Varanasi (after the confluence of the Ganga with the

372 Yamuna) where the chemical composition is intermediate between Himalayan derived

373 sediments and Chambal sediments. Addition of Chambal sediments to Himalayan derived

374   sediments decreases the Na/Si and K/Si ratios and increases the H_2O^+/Si ratio at the outlet and

375   should not be attributed to chemical weathering in the floodplain.

376   Additionally, smaller tributaries draining the Siwaliks were also included in this work

377   as they represent a potential additional source of sediments to the floodplain that is not

378   captured by the trans-Himalayan Rivers sampled at the Himalayan front. Siwalik Rivers show

379   a strong depletion in Na, a high H_2O^+ content and slightly higher Fe content than the other

380   Himalayan Rivers. K on the contrary is similar to other Himalayan Rivers.

381   Finally the Gomti River represents a pure floodplain end member that is more depleted

382   in Na, K and enriched in Fe and H_2O^+ than the Himalayan floodplain Rivers, showing the

383   more weathered state of floodplain material.

384

385   *4.3.3. D/H isotopic composition of sediments*

386

387   The D/H isotopic composition (expressed as δD, ‰ V-SMOW) of the hydroxyls in the

388   sediments from the Ganga basin is not strongly correlated to their degree of hydration (Figure

389   8). However, a shift towards less depleted, higher H_2O^+/Al ratios from the Himalayan front to

390   the Ganga in Bangladesh is obvious. The field of the main hydrated primary minerals, *i.e.*

391   muscovite and biotite have been determined from mono-mineralogical samples from extracted

392   sediments in the Ganga basin (data in supplementary data file, table S2) and are compatible

393   with the previously published analyses on Himalayan source rock minerals (France-Lanord et

394   al., 1988a).

395   The composition of river sediment D/H composition can be explained by a mixing of

396   muscovite and biotite more or less diluted by other aluminosilicates such as feldspar. The

397   analyses of the clay fraction of samples from the Narayani at the Himalayan front and from

398   the Ganga in Bangladesh (Figure 8) as well as the analysis of vermiculite minerals extracted

17

399   from Ganga sediments suggests however that secondary minerals are also significant

400   contributors to the H_2O^+ budget of the samples. The difference in isotopic composition

401   between these clay fractions is at least partly inherited from the difference in the isotopic

402   composition of surface waters in the High Himalayan range and the Gangetic floodplain

403   (respectively ca. – 50 to -135 ‰ and - 20 to - 65 ‰ as determined from river waters by

404   Gajurel et al., 2006). The increase in neo-formation of clay minerals during floodplain

405   transfer is consistent with the change in D/H isotopic composition of the sediments even if a

406   contribution of Chambal derived sediments must also be considered.

407

408   *4.3.4. Carbonates content and isotopic composition*

409

410   Himalayan Rivers and Ganga tributaries are characterized by a large variability in

411   carbonate content (Figure 9). The variability amongst Himalayan basins primarily reflects the

412   regional distribution of carbonated rocks. In Himalayan Rivers, carbonate dissolution during

413   floodplain transit is significant and highly variable amongst rivers (0 to 77 % loss for calcite

414   and 30 to 86 % loss for dolomite). This variability may derive from source effects and/or

415   temporal variations as Himalayan Rivers were not sampled simultaneously. Overall sediments

416   from the Ganga in Bangladesh have low carbonate content compared to sediments from its

417   upstream tributaries with ca. 3% calcite and 2% dolomite (Figure 9).

418

419   The isotopic composition of carbonates is shown in Figure 10 and is in agreement with

420   published data for bedload samples from the Ganga basin (Galy et al., 1999). In addition, the

421   composition of carbonates from Himalayan front Rivers fall within the field of carbonates

422   from Himalayan rocks (France-Lanord, 1987; Galy et al., 1999) supporting their detrital

423   origin. Calcite from Himalayan front Rivers sediments is characterized by a limited range in

424    $\delta^{18}O$ (from ca. -9 to -14 ‰) compared to all available data, while $\delta^{13}C$ values covers the full

425   range of analyzed river sediments in this study. During floodplain transfer these values are

426   shifted towards heavier $\delta^{18}O$ and lighter $\delta^{13}C$ values. Dolomite isotopic composition of

427   Himalayan front Rivers sediments does not show any significant downstream evolution

428   during transfer in the floodplain.

429   Sediments from the Chambal and Siwaliks Rivers have markedly contrasted carbonate

430   isotopic compositions. Carbonates from Chambal sediments are significantly enriched in ^{18}O

431   relative to those from Ganga sediments. In Siwalik Rivers sediments, calcite and dolomite are

432   mainly ^{13}C depleted, which is consistent with Siwalik bulk carbonate isotopic composition

433   (Supplementary data file, table S3; Sanyal et al., 2005). Sediment from the Karnali sampled

434   downstream of the MBT display rather depleted carbonate ^{13}C compositions whereas

435   upstream of the MBT carbonates from Karnali sediments are similar to other Himalayan

436   Rivers sediments. Both calcite and dolomite from Ganga sediments in Bangladesh display

437    $\delta^{13}C$ compositions that are compatible with a mixing of sediments from different Himalayan

438   front Rivers. However, the higher $\delta^{18}O$ values, mainly for calcite, imply the contribution of

439   another source of carbonates, such as Chambal carbonates, pedogenic carbonates from the

440   Gangetic floodplain (Sinha et al., 2006) or biogenic shell carbonates (Gajurel et al., 2006).

441

442   *4.3.5. Mg^s and Ca^s*

443

444   As Mg and Ca concentrations are controlled by both carbonates and silicates, we

445   calculated silicate derived Mg and Ca (noted Mg^s and Ca^s) correcting bulk concentrations for

446   the contribution of carbonate minerals using the measured calcite and dolomite

447   concentrations. Bulk calcium and magnesium concentrations were corrected based

448   contributions of a pure calcite ($CaCO_3$) and dolomite ($Ca_{0.5}Mg_{0.5}CO_3$) component. On

449   average, carbonates account for 28% of the bulk sediment's Mg budget and 73% of the Ca

450   budget.

451   At the first order, calculated Mg^s/Si are positively and linearly correlated to Al/Si

452   ratios ($r^2 > 0.75$; Figure 11a). Scatter is nevertheless large and is most probably induced by

453   uncertainties associated with the dolomite correction. Himalayan front Rivers and Himalayan

454   floodplain Rivers are similar within the data scatter, while the Ganga in Bangladesh

455   consistently shows lower Mg^s/Si ratios than average Himalayan Rivers.

456   The calculated Ca^s/Si ratios span a relatively narrow range in spite of very variable

457   carbonate content (0 to 20 %). This strengthens our confidence in the carbonate correction,

458   because for such a variable carbonate content we would expect a higher range in the case of

459   an inaccurate correction. The calculated Ca^s/Si ratios show no correlation with Al/Si (Figure

460   11b). Within the Ganga basin, the Ca^s/Si ratio does not show a clear downstream evolution

461   during sediment transfer. The Ca^s/Si ratios of Himalayan Rivers sediments are overall very

462   low, which confirms that K, Na and Mg are the dominant silicate cations in the system (Galy

463   and France-Lanord, 1999).

464

465

466   **5. DISCUSSION**

467

468   **5.1. Source effects and temporal variability**

469

470   Sediments in the Ganga basin are characterized by both spatial and temporal

471   variability. To follow and quantify chemical weathering across the entire basin, it is necessary

472   to account for these variations. Inter-basin source effects and contributions from non

473   Himalayan sediments to the total sediment load of the Ganga have to be considered as they

474 would affect the overall sediment composition without being attributable to floodplain

475 weathering.

476

477 *5.1.1. Himalayan tributaries*

478

479 With the exception of carbonates, the chemical composition of Himalayan front Rivers

480 sediments is remarkably homogeneous. Given the contrasted Na/Si and H_2O^+/Si ratios of

481 Himalayan source rocks from different units (Figure 12), this homogeneity suggests that the

482 contribution of the different lithologic units is relatively uniform at the scale of the main

483 Himalayan basins. The notable exception is the Karnali River whose sediments are

484 characterized by lower Na/Si and higher H_2O^+/Si compared to sediments from other trans-

485 Himalayan Rivers.

486 The unusual chemical composition of Karnali sediments could result from higher

487 contributions of sediments from either the Lesser Himalaya or from the Siwalik. Upper

488 Karnali and Behri Rivers sampled upstream of the Siwalik (sample # CA1004-6 and CA1001-

489 3) show higher carbonate $\delta^{13}C$ values than downstream the Siwalik, which suggests a

490 significant contribution of the Siwalik to the Lower Karnali River. Upper Karnali sediments

491 have similar Na/Si ratios than sediments from other trans-Himalayan Rivers. In contrast Behri

492 River sediments are depleted in Na, reflecting a high contribution of LH rocks. Bedload

493 sediments from the Karnali at the Himalayan front also show very low Na/Si ratios,

494 comparable to the Siwalik sediments, a signature that is not observed on the other trans-

495 Himalayan Rivers. A crude mass balance based on the average Na/Si ratios (evaluated for an

496 average Al/Si of 0.22) yields to ca. 25% Siwalik contribution to the total sediment load of the

497 Karnali, assuming that the sediment flux of the Karnali is derived from a mixture of 1/3 of

498 Upper Bheri and 2/3 of sediments equivalent to the Upper Karnali River sediments. Recycling

499   of Siwalik sediments in the Karnali basin was already suggested in a study using apatite

500   fission track in modern sands (Van der Beek et al., 2006), and would be compatible with the

501   high uplift and erosion rates documented during the Holocene for these frontal units (Lavé

502   and Avouac, 2000; 2001).

503   The other trans-Himalayan Rivers drain less Siwaliks and no direct significant Siwalik

504   contribution is observed in their sediments at the front of the Himalayan range. Based on He-

505   Pb dating of zircons, Campbell et al. (2005) also excluded a significant Siwalik contribution

506   to the Ganga. Additional significant contributions of second order rivers draining the southern

507   flank of the Siwalik and contributing to the Ganga sediment load in the floodplain is also

508   unlikely as the high subsidence and accommodation space available in the inter-fan regions of

509   the floodplain would trap large proportions of the sediments transported by these low stream

510   power rivers.

511

512   *5.1.2. Southern tributaries*

513

514   The distinct Fe/Si ratios of the Chambal sediments can be used to trace its contribution

515   to the Ganga sediment load. The linear trend defined by Fe/Si and Al/Si ratios in Himalayan

516   front Rivers is homogeneous and is only slightly affected during floodplain transfer (Figure

517   4). Specifically, Yamuna sediments at the Himalayan front have typical Himalayan

518   compositions. But Yamuna sediments sampled downstream of the confluence with the

519   Chambal are indistinguishable from Chambal sediments (Figure 4, 5, 6, 7) implying that only

520   a minor proportion of the Himalayan Yamuna sediments delivered to the floodplain by the

521   Yamuna River are actually transported through the floodplain, which may have prevailed over

522   the last 120 kyrs (Sinha et al., 2009). This is also consistent with the present day extensive use

523   of water resources in the Western Gangetic plain. Further downstream on the Ganga in

524   Varanasi, the contribution of Chambal sediments is still high. Using the Fe/Si vs. Al/Si

525   relationships of the sediments and assuming a similar grain size distribution for all

526   contributing rivers (similar average Al/Si), we estimate that the contribution of Chambal

527   sediments accounts for ca. 40% of the sediment load in 2001 and 20% in 2008.

528   At the outflow of the Ganga in Bangladesh, the inter-annual variability of sediment

529   composition exceeds the variability observed amongst Himalayan Rivers and can thus only be

530   attributed to the contribution of sediments from the Chambal or other southern tributaries. In

531   2005, unusually high Fe/Si ratios combined with low Na/Si and K/Si ratios suggest a high

532   proportion of Chambal sediments. Conversely, sediments sampled in 2004 are characterized

533   by low Fe/Si ratios and hydration as well as high Na/Si and K/Si ratios. Based on the Al/Si vs

534   Fe/Si regressions defined by sediments collected along depth profiles on the Ganga in

535   Bangladesh it is possible to estimate the contribution of Chambal sediments to the Ganga

536   sediment load. Using the Himalayan floodplain Rivers as a reference, this mass balance

537   calculation shows that the Chambal contributes to up to 17% of the suspended load in

538   Bangladesh in 2005 and ca. 4 % in 2007 and 2008. This estimate assumes that Ganga and

539   Chambal sediments are characterized by a similar average Al/Si of 0.23 (Lupker et al., 2011).

540   We note that the average Al/Si of the Chambal sediment load is not well constrained and that

541   in the event this river mainly contributed to the finer load of the Ganga (i.e. with higher Al/Si)

542   our mass balance calculation would overestimate the Chambal sediment contribution

543   (Supplementary data file, table S4). In 2002, 2004 and 2010 the Fe/Si vs Al/Si trend defined

544   by Ganga sediments is incompatible with mixing between Himalayan floodplain Rivers

545   sediments and Chambal sediments, which excludes a significant Chambal input and points

546   towards second order source effects within the catchments. The contribution of Chambal

547   sediments to the whole Ganga sediment load was also estimated at ca. 5 % based on their

548 relative Sr, Nd and Os isotopic signatures (Singh et al., 2008; Paul, 2008), but these studies do

549 not account for any temporal variability.

550   Variable proportions of Chambal sediments must be accounted for when considering

551 the fate of Himalayan sediments in the system as the composition of Chambal sediments in

552 Na, K and H_2O^+ is very distinct from that of Himalayan sediments. Inter-annual variability of

553 Chambal sediment contribution to the Ganga sediment load also highlights that even in these

554 large systems, the transfer of suspended sediments can be rapid and vary on an annual basis.

555 In spite of its large scale, the Ganga system is thus not fully buffered regarding high

556 frequency variations in its input.

557

558   **5.2. Locus of continental weathering**

559

560 *5.2.1. Quantifying weathering intensity from river sediments*

561

562   To quantitatively assess the role of the Gangetic floodplain in chemical weathering of

563 Himalayan sediments we attempt to characterize and quantify chemical weathering from

564 source to sink. For a given grain size class *i*, the loss or gain in mobile elements *X* normalized

565 to Si ($\Delta X/Si|^i$) can be derived from the difference of composition between upstream and

566 downstream river sediments following eq. (1a):

567 $$\Delta X/Si^i = \left(X/Si\Big|^i_{upstream} - X/Si\Big|^i_{downstream} \right)$$ (1a)

568 because grain-size is strongly correlated to the chemical composition and especially to the

569 Al/Si ratio of sediments (Bouchez et al., 2011b; Lupker et al., 2011), equation (1a) can be

570 rewritten as equation (1b):

571 $$\Delta X/Si^{Al/Si} = \left(X/Si\Big|^{Al/Si}_{upstream} - X/Si\Big|^{Al/Si}_{downstream} \right)$$ (1b)

24

572 Finally, the average loss of mobile elements ($\Delta \overline{X/_{Si}}$) for a given river reach can be determined

573 at the first order, provided that the average Al/Si of the transported sediments is known:

574 $$\Delta \overline{X/_{Si}} = \left(\overline{X/_{Si}}\Big|_{upstream} - \overline{X/_{Si}}\Big|_{downstream} \right) \tag{1c}$$

575 A change in Si concentration during floodplain transfer can occur because of Si dissolution

576 and sequestration of Si-rich material in the floodplain. The dissolved silicon flux in the

577 Himalayan system accounts for only ca. 1% of particulate silicon flux (Galy and France-

578 Lanord, 2001). Furthermore, Lupker et al. (2011) estimated that about 10 % of the Himalayan

579 sediment flux is stored in the floodplain in the form of low Al/Si material. A simple mass

580 balance calculation using the Si content of sediments exported by the Ganga in Bangladesh

581 and the Si content of Ganga bedload as analogue for floodplain material (Lupker et al., 2011)

582 shows that the decrease in Si concentration due to sequestration is limited to less than 2 % of

583 the initial Si content. These two effects are therefore neglected as they remain within the

584 overall uncertainty of the method. The changes in absolute elemental concentrations can thus

585 be approximated to a first order by changes in the silicon-normalized concentrations.

586

587   Based on the sample set presented in this work it is possible to partition the loss of

588 mobile elements between the losses occurring within the Himalayan range (2a), the northern

589 part of the floodplain (2b) and the southern part of the floodplain (2c):

590 $$\Delta \overline{X/_{Si}}\Big|_{HimalayanRange} = \left(\overline{X/_{Si}}\Big|_{HimalayanCrust} - \overline{X/_{Si}}\Big|_{HimalayanFrontRivers} \right) \tag{2a}$$

591 $$\Delta \overline{X/_{Si}}\Big|_{FloodplainN} = \left(\overline{X/_{Si}}\Big|_{HimalayanFrontRivers} - \overline{X/_{Si}}\Big|_{HimalayanFloodplainRivers} \right) \tag{2b}$$

592 $$\Delta \overline{X/_{Si}}\Big|_{FloodplainS} = \left(\overline{X/_{Si}}\Big|_{HimalayanFloodplainRivers} - \overline{X/_{Si}}\Big|_{GangaBangladesh} \right) \tag{2c}$$

593

594   The Himalayan crust composition ($\overline{X/Si}|_{HimalayanCrust}$) is determined from an extensive

595   bedrock sample data set (Galy and France-Lanord, 2001) that we further corrected to include

596   Siwalik sediments (Supplementary data file, Table S6). These estimates only include Na, K

597   and H_2O^+ as for the other elements the unknown distribution and initial content of carbonates

598   in the Himalayan source rocks hampers meaningful estimates. In the floodplain,

599    $\overline{X/Si}|_{HimalayanFrontRivers}$, $\overline{X/Si}|_{HimalayanFloodplainRivers}$ and $\overline{X/Si}|_{GangaBangladesh}$ are determined from averaging $\overline{X/Si}|_i$

600   of each river, i, of the considered reach. $\overline{X/Si}|_i$ is obtained using the relationship between X/Si

601   and Al/Si and the average Al/Si of the sediments. For calcite and dolomite the average

602   compositions are obtained by averaging the carbonate content of all samples available for

603   each river as no correlation with Al/Si is observed. Details of the calculation can be found in

604   Appendix B.

605

606   *5.2.2. Floodplain weathering*

607

608   The evolution of the X/Si ratio in the floodplain is represented in Figure 13. The

609   resulting depletion in mobile elements calculated using equation (2) is given in Table 2. This

610   depletion is computed for Al/Si = 0.23 in the floodplain (c.f. Appendix B). During floodplain

611   transfer from the Himalayan front to the Ganga in Bangladesh sediments mainly loose Na, K

612   and carbonates and gain H_2O^+ relative to silicon even if uncertainties remain high (Figure 13).

613   The loss of Mg^s is limited and bears high uncertainties. For Ca^s, no significant change is

614   observed considering the large uncertainties on average concentrations (Figure 11). Figure 13,

615   shows that for each mole of Na lost in the floodplain, ca. 0.8 mole of K, 0.3 mole of Mg^s, and

616   2 to 3 moles of calcite and dolomite are lost while 1.4 moles of H_2O^+ are gained. Silicate

617   weathering in the Gangetic floodplain mainly releases Na and K, a conclusion already

26

618   attained by dissolved load studies in the system (Sarin et al., 1989; Galy and France-Lanord,

619   1999; Huh, 2010). The absolute K content of Himalayan sediments is ca. 1.5 to 2 times higher

620   than the Na content and the limited loss of K compared to Na therefore highlights the limited

621   mobility of K. Compared to other silicate bound cations, the gain in H_2O^+ is very significant,

622   which makes it a very sensitive proxy for silicate weathering.

623

624   As far as our data set is representative, Na and carbonates are preferentially

625   lost and hydration preferentially gained in the Northern part of the floodplain, between the

626   Himalayan front and the confluence with Ganga mainstream. On average, 70 % of the Na, 60

627   % of the calcite, 80 % of the dolomite depletion and almost 100 % of H_2O^+ gain in the

628   floodplain is observed between the Himalayan front and the Ganga at Harding Bridge has

629   occurred in the first part of the floodplain, which represents, however only ca. 25 % of the

630   total floodplain area drained by the Ganga. K loss is more uniform across the floodplain. This

631   weathering budget of the Himalayan Rivers shows that even a limited floodplain transfer

632   distance (from ca. 590 km for the Ganga and Karnali; 375 km for the Narayani to 200 km for

633   the Kosi) is sufficient to produce a significant weathering signal. This is especially striking in

634   the case of the Narayani River whose floodplain drainage is very limited (ca. 7500 km^2) and

635   does not collect significant sediments from lateral tributaries of the adjacent floodplain or

636   Siwaliks. Using U-series disequilibria, Chabaux et al., 2006 and Granet et al., 2007 estimated

637   that the average transfer time of coarse sediments between the Himalayan front and the

638   confluence with the Ganga eaches up to 100 kyrs for the Karnali and Narayani although fine

639   grain sediments are transferred in less than 25 kyrs (Granet et al., 2010). Long transfer times

640   imply complex interactions exist between the sediments stored in the floodplain and modern

641   river sediments (e.g. Meade et al., 1985; Dunne et al., 1998). Our data suggest that the

642   floodplain / river interactions is a major control of the chemical composition of river

643   sediments. For a similar sediment flux, the upland distributed channels offer a higher active

644   floodplain to river channel ratio promoting exchange between both compartments. The Ganga

645   mainstream on the contrary is bound to a narrower floodplain in the south of the Gangetic

646   plain, which limits interactions. We however emphasize that even if the overall weathering

647   effect of the floodplain on Himalayan sediments is significant, large uncertainties and

648   potential temporal variability may bias our weathering estimates within the floodplain. These

649   caveats should be kept in mind when confronting these results to other studies.

650

651   Gomti River sediments provide a pure floodplain signal as the Gomti River is

652   currently disconnected from any direct Himalayan input (Singh et al., 2005). It cannot be

653   excluded that Gomti sediments originated from "Karnali like" sediments, already depleted in

654   Na. In any case, this river drains alluvial sediments that have experienced weathering for up

655   to 50 kyr (Srivastava et al., 2003). Gomti sediments are depleted in Na compared to Ganga

656   sediments in Bangladesh (Figure 13). But comparatively, K depletion and H_2O^+ gain is

657   limited while Mg^s and Ca^s content is similar to that of Ganga sediments in Bangladesh (Figure

658   10). This is consistent with 1) higher mobility of Na compared to K during floodplain

659   weathering in the Ganga system and 2) the limited loss of silicate Mg and Ca by Himalayan

660   sediments even during very prolonged weathering in the floodplain.

661

662   *5.2.3. Comparison with Himalayan weathering*

663

664   The chemical weathering that occurs in the Gangetic floodplain (section 5.2.2.) can be

665   compared to the weathering of sediments that occurs within the Himalayan range. The latest

666   was determined from equation (2a) for Na, K and H_2O^+ using the composition of Himalayan

667   front Rivers sediments evaluated for Al/Si = 0.22 and the Himalayan crust (Figure 13). This

668   comparison, solely based on the chemical composition of the solid phase in the system shows

669   that 1) Na is mainly lost in the floodplain where ca. 60 % of the total Na loss of the

670   Himalayan system occurs, 2) the loss of K and gain of hydration recorded by the sampled

671   sediments significantly occurs in the floodplain but does not appear significant in the

672   Himalayan range. For K, the apparent loss in the Himalayan range is negligeable. France-

673   Lanord et al. (2003) however show that the dissolved flux of K in the Himalayan front rivers

674   is significant. This highlights that the Himalayan crust composition we use may not be fully

675   representative of the eroded material or that uncertainties are to high to detect a loss of K and

676   gain in H_2O^+. Nevertheless it also suggests that K weathering and hydration in the Himalayan

677   range remains limited while it is significant and resolvable in the floodplain.

678   By using the river sediment composition we show that chemical weathering in the

679   Gangetic floodplain most probably dominates the weathering in the Himalayan range, which

680   is consistent with the conclusions reached by studies of dissolved species in the Himalayan

681   system (Galy and France-Lanord, 1999; West et al., 2002). However, our conclusion relies on

682   the accuracy of the average composition of the eroded Himalayan crust. Evaluating the

683   composition of the Himalayan crust remains a challenging task and is sensitive to sampling

684   biases. Refining the weathering budget from detrital sediments thus requires a better

685   constrains on source rocks composition as already underlined by Gaillardet et al. (1999b).

686

687   *5.2.4. Possible weathering mechanisms*

688

689   Although the purpose of this study is not to determine the exact weathering reactions

690   occurring in the floodplain, the systematic release of Na, K and uptake of OH allow

691   speculating about the possible reactions occurring in the floodplain. Albite being the main Na

692   carrier in Ganga sediments (Garzanti et al., 2011), the release of Na is mainly attributed to its

693   weathering into kaolinite or smectite.

694   K-feldspar dissolution likely represents a source of K. Additionally, abundant

695   vermiculite in floodplain river sediments also supports biotite weathering. The molar K/Mg

696   ratio of Himalayan biotites is ca. 1 (eg. Garzanti et al., 2011; Supplementary data file, Table

697   S7) but during weathering into vermiculites, biotites preferentially loose K, while Mg is

698   immobile or readsorbed as hydrated ion (Velde and Meunier, 2008). This mechanism is

699   supported by semi quantitative SEM-BSE analyses of hand picked biotites and vermiculites

700   showing that K/Al decreases and Mg/Al increases during vermiculitisation (Supplementary

701   data file, Table S7). Muscovite is generally more stable than biotite (e.g. Wilson, 2004) but

702   may also contribute to the dissolved K flux.

703   Increase in hydration is particularly high during clay and hydroxides formation, which

704   is most favorable during longer transfer times in a wet and warm environment such as the

705   Gangetic plain. Tomar (1987), Sarin et al. (1989) and more recently Heroy et al. (2003) and

706   Huyghe et al. (2010), showed the increasing proportion of smectites and other expandable

707   clays over illite from the Himalayan front Rivers to the floodplain Rivers further downstream.

708   This increase in the proportion of secondary minerals in the floodplain is confirmed by both

709   the elemental (H_2O^+/Al) and isotopic (δD) composition of the sediments (Figure 8).

710   Increasing δD values and H_2O^+/Al ratios of the sediments during floodplain transfer reflect

711   the incorporation of a larger proportion of clay minerals in equilibrium with floodplain

712   surface waters, as revealed by the composition of < 2 µm fractions. H_2O^+/Al and δD of

713   detrital sediments are thus indicative of the location of secondary mineral formation.

714   Concerning carbonates, the dissolution rates of calcite and dolomite are surprisingly

715   equivalent. During laboratory experiments, calcite was found to dissolves 5 to 10 times faster

716   than dolomite (eg. Morse and Arvidson, 2002; Prokovsky et al., 2005; Yadav et al., 2008).

717   Szramek et al., 2007 showed, however, using solute chemistry in temperate rivers that the

718   calcite/dolomite dissolution ratio in carbonate bearing watershed reaches 0.6 to 0.7. It has

719   been shown that the Ganga and its tributaries are supersaturated with respect to calcite at least

720   during lean flow (Sarin et al., 1989; Galy and France-Lanord, 1999; Dalai et al., 2002;

721   Jacobson et al., 2002). High dissolved Ca^{2+} concentrations are therefore suspected to hamper

722   calcite dissolution in the floodplain.

723

724   The chemical budgets derived in this work also highlight the different behavior of Na

725   and K. While Na weathering is significant in both the Himalayan range and the Gangetic

726   floodplain, K weathering predominantly occurs in the floodplain. This behavior can be

727   interpreted in the light of the specific weathering rates of the main Na and K bearing minerals,

728   *i.e.* albite and biotite respectively. As Hilley et al., (2010) recently pointed out, the theoretical

729   behavior of minerals with respect to weathering in an erosive context is highly variable and

730   depends on specific weathering rates of each mineral. While considering Himalayan physical

731   erosion rates albite is weathered in supply-limited regime, biotite remains in reaction-limited

732   regime. In the floodplain, lower physical erosion rates or longer residence times (Granet et al.,

733   2010) favor supply-limited regime and high chemical weathering rates for both minerals.

734   These inferences should nevertheless be confirmed by dedicated mineralogical observations.

735

736   **5.3. Floodplain weathering budget**

737

738   The flux of elements weathered in the floodplain and delivered to the dissolved load

739   ($\varphi_X|_{Floodplain}$) is the sum of the flux of elements lost by the sediments during their transfer in

740   the floodplain ($\varphi_X|_{RiverSe\dim ents}$) and by the sediments stored in the floodplain ($\varphi_X|_{StoredSe\dim ents}$):

741   $$\varphi_X|_{Floodplain} = \varphi_X|_{RiverSe\dim ents} + \varphi_X|_{StoredSe\dim ents} \qquad (3)$$

31

742 Reliably assessing the weathering flux associated with the sediments stored in the floodplain

743 remains difficult. The extent of weathering reactions occurring within the sediment column of

744 the floodplain is largely unknown. Furthermore the timescale involved for weathering stored

745 sediments or river sediments is most probably different, which hampers a correct quantitative

746 comparison of both fluxes. However on a qualitative basis this flux remains most probably

747 limited. Floodplain sequestration is limited to ca. 10 % of the Himalayan flux and the average

748 Al/Si of the stored material is low at ca. 0.17 (Lupker et al., 2011). The river sediment data of

749 this work suggests that the loss of mobile elements at lower Al/Si ratios is limited. We

750 therefore suggest here that $\varphi_X\big|_{RiverSe\dim ents} > \varphi_X\big|_{StoredSe\dim ents}$. The floodplain budget presented

751 here is therefore limited to the loss of mobile elements of the sediment load effectively

752 exported by the Ganga basin and may slightly underestimate the complete weathering budget

753 of the floodplain.

754

755   The chemical weathering intensity derived in section 5.2 can therefore be used to

756 estimate the weathering flux of the Gangetic floodplain. Using an average sediment flux (F_{sed})

757 of the Ganga of ca. 400 to 500 Mt/yr (RSP, 1996; Lupker et al., 2011) and an average Si

758 content of Ganga sediments ($\overline{[Si]}$) of ca. 10.6 mol/kg (Lupker et al., 2011) it is possible to

759 estimate the flux of elements transferred from the particulate to the dissolved load during

760 chemical weathering in the floodplain following equation (3):

761       $\varphi_X\big|_{Floodplain} = F_{sed} \cdot \overline{[Si]} \cdot \left(\Delta \overline{X/_{Si}}\big|_{FloodplainS} + \Delta \overline{X/_{Si}}\big|_{FloodplainN} \right)$ (4)

762 Results computed with equation (4) are reported in Table 3. Carbonate Ca and Mg are the

763 main cations released to the dissolved load. Na release is 30 % higher than that of K while

764 Mg^s dissolution flux is limited to less than $20 \cdot 10^9$ moles/yr. Ca^s dissolution flux could not be

765 determined accurately due to the high heterogeneity of sediment composition. But, owing to

766   the lack of significant change and the overall low Ca^s/Si ratios, Ca^s losses can be considered

767   small ($< 10 \cdot 10^9$ moles/yr). These estimates show that weathering can be quantitatively derived

768   from the study of detrital sediments transported by rivers even if calculated fluxes rely on the

769   accurate determination of both total sediment flux and average chemical composition and bear

770   high uncertainties.

771   The weathering fluxes computed from the river sediments in the Ganga plain were

772   compared to the total dissolved fluxes exported out of the basin (Table 3). The dissolved

773   fluxes of the Ganga are taken from Galy and France-Lanord (1999) and corrected for cyclic

774   input. This comparison shows that the weathering fluxes computed in this work are on the

775   same order as total dissolved fluxes currently exported out of the basin. Even if large

776   uncertainties are bound to both estimates this highlights the conclusion drawn above that

777   weathering in the floodplain is significant and probably exceeds weathering in the Himalayan

778   range.

779

780   It should however be noted that $\varphi_X|_{Floodplain}$ deduced from equation (4) only accurately

781   represents the modern weathering flux generated in the floodplain under the assumption that

782   weathering proceeds at steady state. Equation (4) assumes that F_{sed} is constant over the time

783   scale of sediment residence time in the floodplain. Furthermore, any transient change in soil

784   formation/erosion in the floodplain on the time scale of sediment transfer time will lead to an

785   additional sink/source of fine grained sediments within the floodplain that may not have been

786   accounted for and hence may bias $\varphi_X|_{Floodplain}$. This latest has been previously suggested for

787   the Amazon basin, with a recent increase in the export of mature sediments from the

788   floodplain (Gaillardet et al., 1999; Bouchez et al., 2011c) and should be assessed for the

789   Ganga basin in the near future. These limitations should therefore be kept in mind when

790   comparing these weathering fluxes to other estimates such as the dissolved load.

791

6. CONCLUSIONS

793

794   Studying the downstream evolution of the chemical composition of river sediments in

795   the Ganga basin we show that sediments can be used as a quantitative tracer of chemical

796   weathering. Sediment vertical depth profiles show that the chemical variability generated by

797   mineral sorting within the water column exceeds the variability observed among all sampling

798   locations and dates. A single sample is thus merely representative of the sediment flux and

799   cannot be used *a priori* to derive global scale weathering budgets. Using relations between

800   silicon-normalized mobile element concentrations with Al/Si ratios it is possible to derive an

801   average chemical composition for a given river section. Using this approach, we followed the

802   chemical composition of river sediments from the Himalayan front downstream to the Ganga

803   in Bangladesh, across the whole Gangetic floodplain. By integrating the spatial variability

804   among Himalayan tributaries and the temporal variability associated with variable inputs of

805   southern tributaries such as the Chambal, we budget the loss of chemical elements by

806   Himalayan sediments. This budget shows that sediments undergo a significant depletion in

807   Na, K, Ca and Mg that is correlated to a gain in hydration during floodplain transfer.

808   Carbonate dissolution dominates the loss of elements and accounts for respectively ca.

809    $190 \cdot 10^9$ and $70 \cdot 10^9$ mol/yr of Ca and Mg released to the dissolved load. Silicate weathering in

810   the floodplain mainly releases Na and K (ca. $50 \cdot 10^9$ and $40 \cdot 10^9$ mol/yr, respectively). By

811   comparison, the loss of silicate Mg and Ca is limited to less than $20 \cdot 10^9$ and $10 \cdot 10^9$ mol/yr

812   respectively. Weathering in the floodplain is thus significant, but only a limited amount of the

813   produced alkalinity can be attributed to silicate Ca release. Hence, weathering of Himalayan

814   sediments in the Gangetic floodplain is a relatively limited carbon sink, mainly owing to the

815   low Ca silicate content of Himalayan source rocks. Furthermore we show that sediment

816 hydration is a sensitive weathering tracer that can be used in detrital settings, such as the

817 Himalayan system. Comparison of the floodplain weathering budget with the weathering

818 budget obtained by difference with the composition of the Himalayan crust, suggests that

819 silicate weathering is predominantly occurring in the floodplain. However this comparison

820 suffers from the difficulty to accurately assess the source rock composition, specifically for K.

821 A comparison with total dissolved weathering fluxes of the Ganga supports this affirmation

822 even if it should be reminded that these could only be compared under the assumption of

823 steady-state weathering.

824 The chemical composition of river sediments contains a weathering signal that can be

825 quantitatively used to study chemical weathering, provided that first order mineral sorting

826 effects are taken into account. This conclusion supports the use of sedimentary records around

827 the globe for paleo-weathering studies in order to document how surface processes were

828 affected by major geological changes. This work also stresses the need to use a source to sink

829 approach when considering weathering in earth surface systems as in large-scale basins,

830 weathering may not be restricted to high uplift/erosion areas but can also be significantly

831 occurring in the downstream, low land areas.

832

841

APPENDIX A – [H₂O⁺] AND δD REPRODUCTIBILITY

843

844
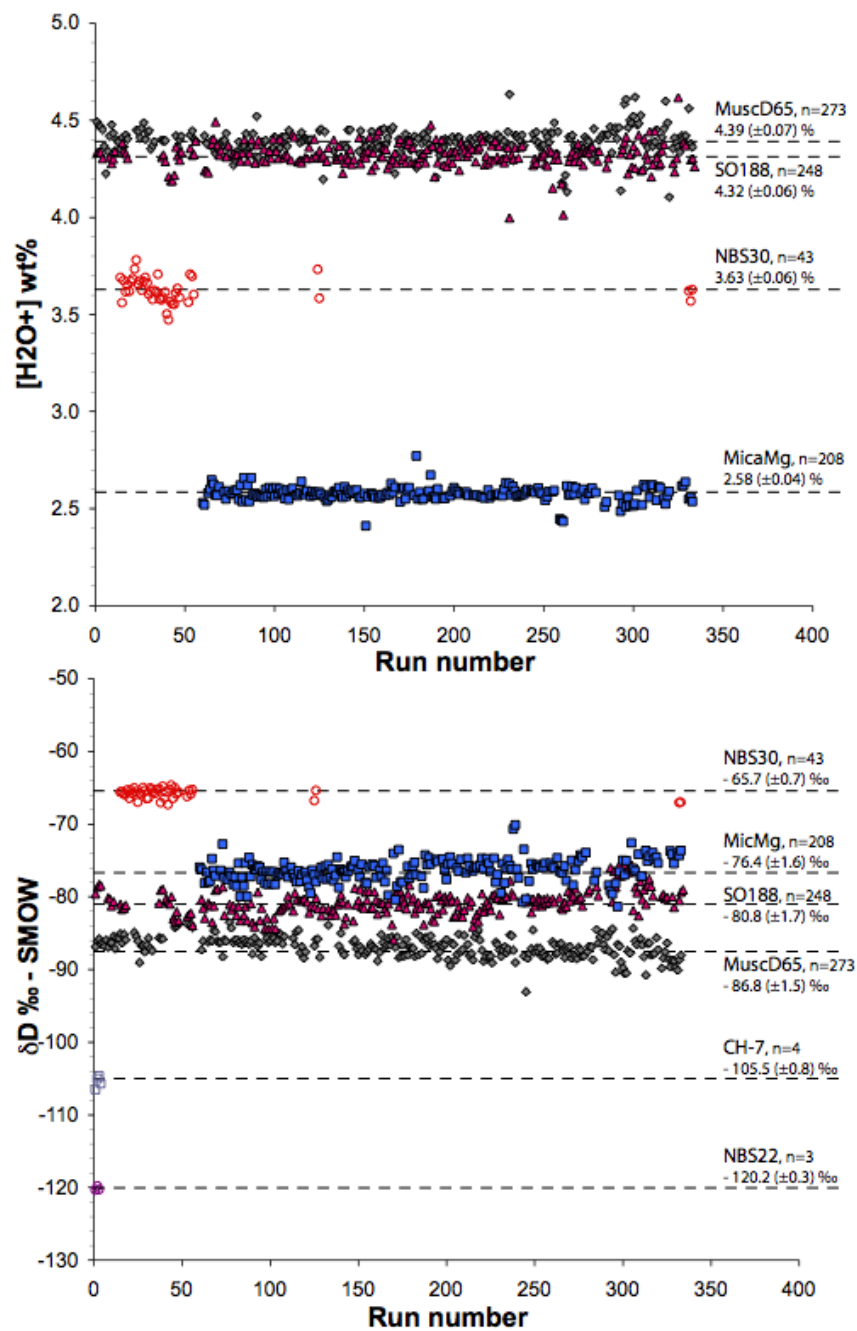
845 **Figure A1:** Replicate analysis of internal standards MuscD65, Mica-Mg and SO188 for H_2O^+

846 concentration (top figure) and D/H isotopic composition (lower figure) routinely measured.

847 Measurements of international reference (NBS 30, NBS 22 and CH-7) are also indicated.

848

849 **APPENDIX B – DETERMINATION OF AVERAGE HIMALAYAN CRUST AND**

850 **SEDIMENT COMPOSITION**

851   The Himalayan crust chemical composition used in this work is derived from the

852 average composition of HHC and LH rocks as compiled by Galy and France-Lanord (2001),

853 with the addition of samples from Pecher (1978) and Brouand (1987). The average Nd

854 isotopic composition of Himalayan sediments indicates that ca. 80 % of sediments are derived

855 from the HHC and 20 % from LH (Galy and France-Lanord, 2001). We further corrected this

856 estimate for Siwalik contribution as the Siwalik represent a source of sediments to the

857 Gangetic system that must be accounted for (see section 5.1.1.). Lavé and Avouac (2001)

858 have estimated the relative contribution of Siwalik sediment to ca. 15 to 20 % of the total

859 sediment flux. However, those fluxes are in large part deposited in the Ganga plain between

860 the mega fans of the main transhimalayan Rivers, so that we arbitrarily estimated that only ca.

861 10 % of sediments transported by the floodplain Rivers are from Siwalik origin. Therefore

862 $\left.\overline{X/Si}\right|_{HimalayanCrust}$ is given by equation (B1):

863 $$\left.\overline{X/Si}\right|_{HimalayanCrust} = 0.72\cdot \left.\overline{X/Si}\right|_{HHC} + 0.18\cdot \left.\overline{X/Si}\right|_{LH} + 0.10\cdot \left.\overline{X/Si}\right|_{Siwaliks} \qquad (B1)$$

864 Uncertainties on source rock composition and on the relative proportions of each geological

865 unit are propagated through the calculation (c.f. supplementary data, Table S6).

866

867   For the Himalayan front and floodplain river sediments, $\left.\overline{X/Si}\right|_{HimalayanFrontRivers}$ and

868 $\left.\overline{X/Si}\right|_{HimalayanFloodplainRivers}$ are determined from chemical composition of each river of the reach,

869 $\left.\overline{X/Si}\right|_{i}$ (e.g. he Yamuna, Ganga, Karnali, Narayni and Kosi for the Himalayan front) weighted

870 by its respective sediment flux, F_i:

871 $$\left.\overline{X/Si}\right|_{HimalayanFrontRivers, HimalayaFloodplainRivers} = \frac{1}{\sum_i F_i}\cdot \sum_i F_i\cdot \left.\overline{X/Si}\right|_{i} \qquad (B2)$$

872   Fluxes are mainly derived from sediment gauging data (HMG, Nepal Electr. Author., 1982;

873   Ghimire and Uprety, 1990; Sinha and Friend, 1994) or from cosmo-nuclides derived erosion

874   rates (Vance et al., 2003). We conservatively propagated 50 % uncertainty on these fluxes.

875   For the Ganga in Bangladesh, $\overline{X/Si}\big|_{GangaBangladesh}$ was determined from averaging each sampling

876   year after correction for potential Chambal sediment contribution (as discussed in section

877   5.1.2):

878        $$\overline{X/Si}\big|_{GangaBangladesh} = \frac{1}{i} \cdot \sum_i \overline{X/Si_{corrected}}\big|_i \qquad\qquad\qquad\text{(B3)}$$

879

880   For all river sediments, $\overline{X/Si}\big|_i$ was determined through the regression between, X/Si and

881   Al/Si (linear for Fe, K, H_2O^+ and Mg^s and logarithmic for Na, c.f. Figure 4, 5, 6, 7 and 11)

882   and the average Al/Si of the sediments. Because the chemical composition of bedload samples

883   is affected by placer effects and because these bedload samples have a strong control on the

884   regression between Al/Si and X/Si, we chose to force the regressions through a uniform

885   bedload composition obtained after averaging all available bedloads in the Ganga floodplain.

886   This is justified, as even if the bedload composition is variable between sampling sites or

887   dates, there is no significant and systematic evolution in bedload composition in the

888   floodplain. When considering Himalayan weathering, the averaged Al/Si used to determine

889    $\overline{X/Si}\big|_i$ is 0.22 as this is the average Al/Si determined for the Himalayan crust and for Himalayan

890   front River sediments (Lupker et al., 2011). When considering floodplain weathering, the

891   average Al/Si used is 0.23 as the average material that is effectively transported through the

892   entire Ganga floodplain has a ratio of 0.23 due due to sediment sequestration in the floodplain

893   (Lupker et al., 2011). For calcite and dolomite content, $\overline{X/Si}\big|_i$ is obtained by averaging the

894   composition of all available samples of a given river as no relation to Al/Si is found.

895

896 **References**

897 Attal, M. and Lave, J., 2006. Changes of bedload characteristics along the Marsyandi River

898   (central Nepal): Implications for understanding hillslope sediment supply, sediment

899   load evolution along fluvial networks, and denudation in active orogenic belts. In:

900   Willett, S. D., Hovius, N., Brandon, M. T., and Fisher, D. M. Eds.), Tectonics,

901   climate, and landscape evolution.

902 Berner, R., Lasaga, A., and Garrels, R., 1983. The carbonate-silicate geochemical cycle and

903   its effect on atmospheric carbon dioxide over the past 100 million years. *Am. J. Sci*

904   **283**, 641–683.

905 Berner, R. A., 1994. GEOCARB-II - A Revised Model of Atmospheric CO2 over

906   Phanerozoic Time. *American Journal of Science* **294**, 56-91.

907 Bigeleisen, J. L., Perlman, M., and Prosser, H. C., 1952. Conversion of hydrogenic material to

908   hydrogen for isotopic analyses. *Analytical Chemistry* **24**, 1356-1357.

909 Bouchez, J., Metivier, F., Lupker, M., Maurice, L., Perez, M., Gaillardet, J., and France-

910   Lanord, C., 2011a. Prediction of depth-integrated fluxes of suspended sediment in the

911   Amazon River: particle aggregation as a complicating factor. *Hydrological Processes*

912   **25**, 778-794.

913 Bouchez, J., Gaillardet, J., France-Lanord, C., Maurice, L., and Dutra-Maia, P., 2011b. Grain

914   size control of river suspended sediment geochemistry: Clues from Amazon River

915   depth profiles. *Geochem. Geophys. Geosyst.* **12**, Q03008.

916 Bouchez, J., Lupker, M., Gaillardet, J., France-Lanord, C., and Maurice, L., 2011c. How

917   important is it to integrate riverine suspended sediment chemical composition with

918   depth? Clues from Amazon River depth-profiles. *Geochimica Et Cosmochimica Acta*

919   **75**, 6955-6970.

920 Brouand, M., 1987. Pétrogenèse des migmatites de la dalle du tibet (Himalaya du Népal),

921   Insitut National Polytechnique de Lorraine (INPL) – Nancy, 366p.

922   Burgoyne, T. W. and Hayes, J. M., 1998. Quantitative Production of H2 by Pyrolysis of Gas

923   Chromatographic Effluents. *Analytical Chemistry* **70**, 5136-5141.

924   Campbell, I. H., Reiners, P. W., Allen, C. M., Nicolescu, S., and Upadhyay, R., 2005. He–Pb

925   double dating of detrital zircons from the Ganges and Indus Rivers: Implication for

926   quantifying sediment recycling and provenance studies. *Earth and Planetary Science*

927   *Letters*, 402-432.

928   Carignan, J., Hild, P., Mevelle, G., Morel, J., and Yeghicheyan, D., 2001. Routine analyses of

929   trace elements in geological samples using flow injection and low pressure on-line

930   liquid chromatography coupled to ICP-MS: A study of geochemical reference

931   materials BR, DR-N, UB-N, AN-G and GH. *Geostandards Newsletter-the Journal of*

932   *Geostandards and Geoanalysis* **25**, 187-198.

933   Chabaux, F., Granet, M., Pelt, E., France-Lanord, C., and Galy, V., 2006. U-238-U-234-Th-

934   230 disequilibria and timescale of sedimentary transfers in rivers: Clues from the

935   Gangetic plain rivers. *Journal of Geochemical Exploration* **88**, 373-375.

936   Dalai, T. K., Krishnaswami, S., and Sarin, M. M., 2002. Major ion chemistry in the

937   headwaters of the Yamuna river system: : Chemical weathering, its temperature

938   dependence and CO2 consumption in the Himalaya. *Geochimica Et Cosmochimica*

939   *Acta* **66**, 3397-3416.

940   Donnadieu, Y., Goddéris, Y., Ramstein, G., Nédélec, A., and Meert, J., 2004. A 'snowball

941   Earth'climate triggered by continental break-up through changes in runoff. *Nature*

942   **428**, 303-306.

943   Dunne, T., Mertes, L. A. K., Meade, R. H., Richey, J. E., and Forsberg, B. R., 1998.

944   Exchanges of sediment between the flood plain and channel of the Amazon River in

945   Brazil. *Geological Society of America Bulletin* **110**, 450-467.

946   Fasullo, J. and Webster, P. J., 2003. A hydrological definition of Indian monsoon onset and

947   withdrawal. *Journal of Climate* **16**, 3200-3211.

948   France-Lanord, C., 1987. Chevauchement, métamorphisme et magmatisme en Himalaya du

949   Népal central. Etude isotopique H, C, O. Thèse, Institut National Polytechnique de

950   Lorraine.

951   France-Lanord, C., Sheppard, S. M. F., and Le Fort, P., 1988. Hydrogen and oxygen isotope

952   variations in the High Himalaya peraluminous Manaslu leucogranite : evidence for

953   heterogeneous sedimentary sources. *Geochimica et Cosmochimica Acta* **52**, 513-526.

954   France-Lanord, C. and Derry, L. A., 1997. Organic carbon burial forcing of the carbon cycle

955   from Himalayan erosion. *Nature* **390**, 65-67.

956   France-Lanord, C., Evans, M., Hurtrez, J. E., and Riotte, J., 2003. Annual dissolved fluxes

957   from Central Nepal rivers: budget of chemical erosion in the Himalayas. *Comptes*

958   *Rendus Geoscience* **335**, 1131-1140.10.1016/j.crte.2003.09.014|ISSN 1631-0713

959   Gaillardet, J., Dupré, B., and Allègre, C. J., 1999. Geochemistry of large river suspended

960   sediments: silicate weathering or recycling tracer? *Geochimica Et Cosmochimica Acta*

961   **63**, 4037-4051.

962   Gaillardet, J., Dupré, B., Louvat, P., and Allègre, C. J., 1999. Global silicate weathering and

963   CO2 consumption rates deduced from the chemistry of large rivers. *Chemical Geology*

964   **159**, 3-30.

965   Gajurel, A. P., 1998. Géochimie isotopique et déformations synsédimentaires des dépôts du

966   bassin de Kathmandou. DEA, Université Joseph Fourier.

967   Galy, A. and France-Lanord, C., 1999. Weathering processes in the Ganges-Brahmaputra

968   basin and the riverine alkalinity budget. *Chemical Geology* **159**, 31-60.

969   Galy, A. and France-Lanord, C., 2001. Higher erosion rates in the Himalaya: Geochemical

970   constraints on riverine fluxes. *Geology* **29**, 23-26.

971   Galy, A., France-Lanord, C., and Derry, L. A., 1999. The strontium isotopic budget of
972   Himalayan Rivers in Nepal and Bangladesh. *Geochimica Et Cosmochimica Acta* **63**,
973   1905-1925.

974   Galy, V., France-Lanord, C., Beyssac, O., Faure, P., Kudrass, H., and Palhol, F., 2007.
975   Efficient organic carbon burial in the Bengal fan sustained by the Himalayan erosional
976   system. *Nature* **450**, 407-U6.

977   Galy, V., France-Lanord, C., and Lartiges, B., 2008. Loading and fate of particulate organic
978   carbon from the Himalaya to the Ganga-Brahmaputra delta. *Geochimica et*
979   *Cosmochimica Acta* **72**, 1767–1787.

980   Garzanti, E., Ando, S., France-Lanord, C., Censi, P., Vignola, P., Galy, V., and Lupker, M.,
981   2011. Mineralogical and chemical variability of fluvial sediments 2. Suspended-load
982   silt (Ganga-Brahmaputra, Bangladesh). *Earth and Planetary Science Letters* **302**, 107-
983   120.

984   Garzanti, E., Ando, S., France-Lanord, C., Vezzoli, G., Censi, P., Galy, V., and Najman, Y.,
985   2010. Mineralogical and chemical variability of fluvial sediments: 1. Bedload sand
986   (Ganga-Brahmaputra, Bangladesh). *Earth and Planetary Science Letters* **299**, 368-
987   381.

988   Garzione, C. N., Hoke, G. D., Libarkin, J. C., Withers, S., MacFadden, B., Eiler, J., Ghosh,
989   P., and Mulch, A., 2008. Rise of the Andes. *Science* **320**, 1304-1307.

990   Gehre, M. and Strauch, G., 2003. High-temperature elemental analysis and pyrolysis
991   techniques for stable isotope analysis. *Rapid Communications in Mass Spectrometry*
992   **17**, 1497-1503.

993   Ghimire, G. and Uprety, B., 1990. Causes and effects of siltation on the environment of
994   Nepal. *The Environmentalist* **10**, 55-65.

995   Gilg, H. A. and Sheppard, S. M. F., 1996. Hydrogen isotope fractionation between kaolinite

996   and water revisited. *Geochimica Et Cosmochimica Acta* **60**, 529-533.

997   Girard, J. P., Freyssinet, P., and Chazot, G., 2000. Unraveling climatic changes from

998   intraprofile variation in oxygen and hydrogen isotopic composition of goethite and

999   kaolinite in laterites: An integrated study from Yaou, French Guiana. *Geochimica Et*

1000   *Cosmochimica Acta* **64**, 409-426.

1001   Gislason, S. R., Oelkers, E. H., and Snorrason, A., 2006. Role of river-suspended material in

1002   the global carbon cycle. *Geology* **34**, 49-52.

1003   Gong, B., Zheng, Y. F., and Chen, R. X., 2007. TC/EA-MS online determination of hydrogen

1004   isotope composition and water concentration in eclogitic garnet. *Physics and*

1005   *Chemistry of Minerals* **34**, 687-698.

1006   Govindaraju, K. and Mevelle, G., 1987. Fully automated dissolution and separation methods

1007   for inductively coupled plasma atomic emission-spectrometry rock analysis –

1008   application to the determination of rare-earth elements. *Journal of Analytical Atomic*

1009   *Spectrometry* **2**, 615-621.

1010   Granet, M., Chabaux, F., Stille, P., Dosseto, A., France-Lanord, C., and Blaes, E., 2010. U-

1011   series disequilibria in suspended river sediments and implication for sediment transfer

1012   time in alluvial plains: The case of the Himalayan rivers. *Geochimica Et*

1013   *Cosmochimica Acta* **74**, 2851-2865.

1014   Granet, M., Chabaux, F., Stille, P., France-Lanord, C., and Pelt, E., 2007. Time-scales of

1015   sedimentary transfer and weathering processes from U-series nuclides: Clues from the

1016   Himalayan rivers. *Earth and Planetary Science Letters* **261**, 389-406.

1017   Heroy, D. C., Kuehl, S. A., and Goodbred, S., 2004. Mineralogy of the Ganges and

1018   Brahmaputra Rivers: implications for river switching and Late Quaternary climate

1019   change. *Sedimentary Geology* **155**, 343–359.

1020   Hilley, G. E., Chamberlain, C. P., Moon, S., Porder, S., and Willett, S. D., 2010. Competition

1021   between erosion and reaction kinetics in controlling silicate-weathering rates. *Earth*

1022   *and Planetary Science Letters* **293**, 191-199.

1023   HMG, 1994. His Majesty's Government of Nepal - Middle Marsyandi Hydroelectric Project,

1024   Nepal Electr. Author.

1025   Huh, Y., 2010. Estimation of atmospheric CO2 uptake by silicate weathering in the

1026   Himalayas and the Tibetan Plateau: a review of existing fluvial geochemical data

1027   *Geological Society London Special Publications* **342**, 129-151.

1028   Huyghe, P., Guilbaud, R., Bernet, M., Galy, A., and Gajurel, A. P., 2010. Significance of the

1029   clay mineral distribution in fluvial sediments of the Neogene to Recent Himalayan

1030   Foreland Basin (west-central Nepal). *Basin Research*, no-no.

1031   Jacobson, A. D., Blum, J. D., and Walter, L. M., 2002. Reconciling the elemental and Sr

1032   isotope composition of Himalayan weathering fluxes; insights from the carbonate

1033   geochemistry of stream waters. *Geochimica et Cosmochimica Acta* **66**, 3417-3429.

1034   Lave, J. and Avouac, J. P., 2000. Active folding of fluvial terraces across the Siwaliks Hills,

1035   Himalayas of central Nepal. *Journal of Geophysical Research, B, Solid Earth and*

1036   *Planets* **105**, 5735-5770.

1037   Lavé, J. and Avouac, J. P., 2001. Fluvial incision and tectonic uplift across the Himalayas of

1038   central Nepal. *J. Geophys. Res.* **106**, 26561.

1039   Lawrence, J. R. and Taylor, H. P., 1971. Deuterium and oxygen-18 correlation : clay minerals

1040   and hydroxides in quaternary soils compared to meteoric waters. *Geochimica et*

1041   *Cosmochimica Acta* **35**, 993-1003.

1042   Lawrence, J. R. and Taylor, H. P., 1972. Hydrogen and oxygen isotope systematics in

1043   weathering profiles. *Geochimica Et Cosmochimica Acta* **36**, 1377-&.

1044   Lupker, M., France-Lanord, C., Lavé, J., Bouchez, J., Galy, V., Métivier, F., Gaillardet, J.,

1045   Lartiges, B., and J.-L. Mugnier, 2011. A Rouse-based method to integrate the

1046	chemical composition of river sediments: application to the Ganga basin. *J. Geophys.*

1047	*Res*. doi : 10.1029/2010JF001947

1048	Lyon-Caen, H. and Molnar, P., 1983. Constraints on the structure of the Himalaya from an

1049	analysis of gravity anomalies and a flexural model of the lithsophere. *Journal of*

1050	*Geophysical Research* **88**, 8171-8191.

1051	Meade, R. H., Dunne, T., Richey, J. E., Santos, U. D., and Salati, E., 1985. Storage and

1052	remobilization of suspended sediment in the lower Amazon River of Brazil. *Science*

1053	**228**, 488-490.

1054	Meybeck, M., 1987. Global chemical weathering of surficial rocks estimated from river

1055	dissolved loads. *American Journal of Science* **287**, 401-428.

1056	Morse, J. W. and Arvidson, R. S., 2002. The dissolution kinetics of major sedimentary

1057	carbonate minerals. *Earth-Science Reviews* **58**, 51-84.

1058	Oelkers, E. H. and Schott, J., 1995. Experimental study of anorthite dissolution and the

1059	relative mechanism of feldspar hydrolysis. *Geochimica Et Cosmochimica Acta* **59**,

1060	5039-5053.

1061	Paul, M., 2008. Etude des isotopes de l'osmium dans les eaux souterraines du Bangladesh et

1062	les sédiments himalayens: implications et rôle de l'érosion himalayenne sur le budget

1063	océanique de l'osmium., Doctorat Géosciences, INPL Nancy - France

1064	Pecher, A., 1978. Deformation et metamorphisme associés à une zone de cisaillement.

1065	Exemple du grand chevauchement central himalayen (M.C.T.), transverale des

1066	Annapurnas et du Manaslu, Nepal. Thèse Sci., Grenoble, 354p.

1067	Pokrovsky, O. S., Golubev, S. V., and Schott, J., 2005. Dissolution kinetics of calcite,

1068	dolomite and magnesite at 25 ∞C and 0 to 50 atm pCO2. *Chemical Geology* **217**, 239-

1069	255.

1070	Rao, K. L., 1979. *India's water wealth*. Orient Longman limited, New Delhi.

1071   Raymo, M. E., Ruddiman, W. F., and Froelich, P. N., 1988. Influence of late Cenozoic

1072   mountain building on ocean geochemical cycles. *Geology* **16**, 649-653.

1073   Rengarajan, R., Singh, S. K., Sarin, M. M., and Krishnaswami, S., 2009. Strontium isotopes

1074   and major ion chemistry in the Chambal River system, India: Implications to silicate

1075   erosion rates of the Ganga. *Chemical Geology* **260**, 87-101.

1076   RSP, 1996. River Survey Project, Flood Action Plan (FAP) final report. Delft Hydraulics and

1077   DHI.

1078   Sanyal, P., Bhattacharya, S. K., and Prasad, M., 2005. Chemical diagenesis of Siwalik

1079   sandstone: Isotopic and mineralogical proxies from Surai Khola section, Nepal.

1080   *Sedimentary Geology* **180**, 57-74.

1081   Sarin, M. M., Krishnaswami, S., Dilli, K., Somayajulu, B. L. K., and Moore, W. S., 1989.

1082   Major ion chemistry of the Ganga-Brahmaputra river system: Weathering processes

1083   and fluxes to the Bay of Bengal. *Geochimica et Cosmochimica Acta* **53**, 997-1009.

1084   Savin, S. M. and Epstein, S., 1970. Oxygen and hydrogen isotope geochemistry of lcay

1085   minerals. *Geochimica Et Cosmochimica Acta* **34**, 25-&.

1086   Sharp, Z. D., Atudorei, V., and Durakiewicz, T., 2001. A rapid method for determination of

1087   hydrogen and oxygen isotope ratios from water and hydrous minerals. *Chemical

1088   Geology* **178**, 197-210.

1089   Sheppard, S. M. F. and Schwarcz, H. P., 1970. Fractionation of carbon and oxygen isotopes

1090   and magnesium between coexisting metamorphic calcite and dolomite. *Contributions

1091   to Mineralogy and Petrology* **26**, 161-198.

1092   Singh, M., Sharma, M., and Tobschall, H. J., 2005. Weathering of the Ganga alluvial plain,

1093   northern India: implications from fluvial geochemistry of the Gomati River. *Applied

1094   Geochemistry*, 1-21.

1095   Singh, S. K., Rai, S. K., and Krishnaswami, S., 2008. Sr and Nd isotopes in river sediments

1096   from the Ganga Basin: Sediment provenance and spatial variability in physical

1097   erosion. *J. Geophys. Res.* **113**, F03006.

1098   Sinha, R. and Friend, P. F., 1994. River systems and their sediment flux, Indo-Gangetic

1099   plains, northern Bihar, India. *Sedimentology* **41**, 825-845.

1100   Sinha, R., Kettanah, Y., Gibling, M. R., Tandon, S. K., Jain, M., Bhattacharjee, P. S.,

1101   Dasgupta, A. S., and Ghazanfari, P., 2009. Craton-derived alluvium as a major

1102   sediment source in the Himalayan Foreland Basin of India. *Geological Society of*

1103   *America Bulletin* **121**, 1596-1610.

1104   Sinha, R., Tandon, S. K., Sanyal, P., Gibling, M. R., Stuben, D., Berner, Z., and Ghazanfari,

1105   P., 2006. Calcretes from a Late Quaternary interfluve in the Ganga Plains, India:

1106   Carbonate types and isotopic systems in a monsoonal setting. *Palaeogeography,*

1107   *Palaeoclimatology, Palaeoecology* **242**, 214-239.

1108   Srivastava, P., Singh, I. B., Sharma, M., and Singhvi, A. K., 2003. Luminescence

1109   chronometry and Late Quaternary geomorphic history of the Ganga Plain, India.

1110   *Palaeogeography, Palaeoclimatology, Palaeoecology* **197**, 15-41.

1111   Szramek, K., McIntosh, J. C., Williams, E. L., Kanduc, T., Ogrinc, N., and Walter, L. M.,

1112   2007. Relative weathering intensity of calcite versus dolomite in carbonate-bearing

1113   temperate zone watersheds: Carbonate geochemistry and fluxes from catchments

1114   within the St. Lawrence and Danube river basins. *Geochem. Geophys. Geosyst.* **8**,

1115   Q04002.

1116   Tomar, K. P., 1987. Chemsitry of pedogenesis in Indo-Gangetic alluvial plains. *Journal of*

1117   *Soil Science* **38**, 405-414.

1118   Van Der Beek, P., Robert, X., Mugnier, J.-L., Bernet, M., Huyghe, P., and Labrin, E., 2006.

1119   Late Miocene ? Recent exhumation of the central Himalaya and recycling in the

1120   foreland basin assessed by apatite fission-track thermochronology of Siwalik

1121   sediments, Nepal. *Basin Research* **18**, 413-434.

1122   Vance, D., Bickle, M., Ivy-Ochs, S., and Kubik, P. W., 2003. Erosion and exhumation in the

1123   Himalaya from cosmogenic isotope inventories of river sediments. *Earth and*

1124   *Planetary Science Letters* **206**, 273-288.

1125   Velde, B. B. and Meunier, A., 2008. The Origin of Clay Minerals in Soils and Weathered

1126   Rocks. Springer.

1127   Walker, J. C. G., Hays, P. B., and Kasting, J. F., 1981. A negative feed back mechanism for

1128   the long-term stabilization of Earth's surface temperature. *Journal of Geophysical*

1129   *Research* **86**, 9776-9782.

1130   WARPO, Water Resources Planning Organization, Ministry of water resources, Government

1131   of the People's Republic of Bangladesh. Hydrological data.

1132   West, A. J., Bickle, M. J., Collins, R., and Brasington, J., 2002. Small-catchment perspective

1133   on Himalayan weathering fluxes. *Geology* **30**, 355-358.

1134   West, A. J., Galy, A., and Bickle, M., 2005. Tectonic and climatic controls on silicate

1135   weathering. *Earth and Planetary Science Letters* **235**, 211-228.

1136   White, A. F. and Brantley, S. L., 2003. The effect of time on the weathering of silicate

1137   minerals: why do weathering rates differ in the laboratory and field? *Chemical*

1138   *Geology* **202**, 479-506.

1139   Wilson, M. J., 2004. Weathering of the primary rock-forming minerals: processes, products

1140   and rates. *Clay Minerals* **39**, 233-266.

1141   Yadav, S., Chakrapani, G., and Gupta, M., 2008. An experimental study of dissolution

1142   kinetics of Calcite, Dolomite, Leucogranite and Gneiss in buffered solutions at

1143   temperature 25 and 5°C. *Environmental Geology* **53**, 1683-1694.

1144   Yapp, C. J. and Pedley, M. D., 1985. Stable Hydrogen isotopes in iron-oxides. 2. D/H

1145   variations among natural Goethites. *Geochimica Et Cosmochimica Acta* **49**, 487-495.

1146

Figures

Figure 1: Geographical setting of the Ganga basin showing the main sample sites and

corresponding sample numbers. A geological sketch of the main Himalayan faults zones is

also shown (ITS: Indus-Tsangpo Suture; STD: South Tibetan Detachment; MCT: Main

Central Thrust; MBT: Main Boundary Thrust; MFT: Main Frontal Thrust).

Figure 2: Evolution of sediment concentration in the water column of the Ganga in

Bangladesh (BR 511 - 516) along with the evolution of the chemical composition of major

elements Si, Al, Fe, Na, K as well as H_2O^+. Mineral sorting within the water column is a first

order control on the chemical composition of sampled sediments (Lupker et al., 2011;

Bouchez et al., 2011b).

Figure 3: Schematic evolution of the sedimentary load during transfer from the Himalayan

front downstream to the Ganga in Bangladesh. (a) Sediment hydrodynamic sorting results in

mixing trend between coarse grained, quartz rich, low Al/Si sediments and a clay and

phyllosilicate rich end-member. Weathering is marked by a loss of mobile elements (e.g. K,

Na, …) relative to Si at constant Al/Si. (b) Sediment sequestration in the floodplain results in

a relative increase of the average Al/Si ratio of the total transported sediment load. This

evolution is however limited for the Ganga as at the Himalayan front the average Al/Si is ca.

0.22 and in the Ganga in Bangladesh this ratio is estimated at ca. 0.23 (Lupker et al., 2011).

Figure 4: a. Evolution of the Fe/Si ratio as a function of the Al/Si ratio, proxy for grain-size

and mineral sorting in the river water column. Himalayan Rivers form a relatively uniform

trend that is markedly different from sediments from the southern tributaries such as the

1172 Chambal. This difference can be used to trace inputs from Chambal sediments in sediments

1173 from the Ganga mainstream. **b.** Detailed graph of the Himalayan front rivers. **c.** Temporal of

1174 Fe/Si ratios of sediments sampled in the Ganga in Bangladesh, plotted as a function of

1175 sampling year, highlighting the heterogeneity of the exported chemical signal.

1176

1177 **Figure 5: a.** Evolution of the Na/Si ratio as a function of the Al/Si ratio, showing a depletion

1178 in Na relative to Si from the Himalayan front Rivers (black squares) downstream to the

1179 Himalayan floodplain Rivers (light grey diamonds) and the Ganga in Bangaldesh (open

1180 circles). **b.** Composition variability amongst Himalayan front Rivers showing a Na-depleted

1181 Karnali compared to other Himalayan Rivers **c.** Inter-annual variability of the Na/Si ratio in

1182 Ganga sediments sampled in Bangladesh.

1183

1184 **Figure 6:** Evolution of the K/Si ratio as a function of the Al/Si ratio, showing a depletion in K

1185 from the Himalayan front Rivers (black squares) downstream to the Himalayan floodplain

1186 Rivers (light grey diamonds) and the Ganga in Bangaldesh (open circles). **b.** Himalayan front

1187 River sediments have homogeneous K/Si composition **c.** Inter-annual variability of the K/Si

1188 ratio in Ganga sediments sampled in Bangladesh.

1189

1190 **Figure 7:** Evolution of the H_2O^+/Si ratio as a function of the Al/Si ratio. **a.** Evolution of

1191 H_2O^+/Si from the Himalayan front rivers (black squares), further downstream upon floodplain

1192 transfer (light grey diamonds) compared to Ganga sediments sampled in Bangladesh (open

1193 circles) and the major southern contribution of the Chambal (black triangles). **b.** Detailed plot

1194 of the evolution of Himalayan rivers upon floodplain transfer. **c.** Inter-annual variability of the

1195 H_2O^+/Si ratio in Ganga sediments sampled in Bangladesh.

1196

1197   **Figure 8:** D/H isotopic composition of bulk sediments from the Ganga basin as a function of

1198   hydration expressed as the H_2O^+/Al ratio. The hydration and isotopic composition of

1199   muscovite, biotite and vermiculite separated from Himalayan sediments (see supplementary

1200   data file, Table S2) is also plotted for references.

1201

1202   **Figure 9:** Calcite and dolomite content of sediments from the Ganga basin.

1203

1204   **Figure 10:** Oxygen and carbon isotopic composition of calcite (a) and dolomite (b) of river

1205   sediments from the Ganga basin. The range of composition of pedogenic carbonates from the

1206   northeastern Ganga floodplain (Sinha et al., 2006), Siwaliks carbonates from the Surai Khola

1207   section in Nepal (Suppelmentary data file, Table S3; Sanyal et al., 2005), biogenic shells from

1208   the Gangetic plain (Gajurel et al., 2006) and Himalayan source rocks (Galy et al., 1999) is

1209   also shown.

1210

1211   **Figure 11:** Mg^s/Si (a) and Ca^s/Si ratio (b) as a function of Al/Si ratio for river sediments from

1212   the Himalayan front Rivers, the Himalayan flood plain Rivers, the Ganga in Bangladesh, the

1213   Chambal and Gomti Rivers. Mg^s and Ca^s are derived from the sediment bulk Mg and Ca

1214   content after correction for calcite and dolomite Ca and Mg contribution.

1215

1216   **Figure 12:** Na/Si, K/Si and H_2O^+/Si ratios of the main lithological units of the Himalayan

1217   orogen: Siwaliks, Lesser Himalaya (LH) and High Himalaya Cristalines (HHC). The

1218   chemical composition of these units are from Galy and France-Lanord (2001) and Lupker et

1219   al. (2011) and are based on outcrop samples.

1220

1221   **Figure 13:** Evolution of the normalized mobile element composition of sediments in the

1222   Himalayan system. Weathering in the Himalayan range (green envelope) is computed for an

1223   average Al/Si ratio of 0.22. Weathering in the floodplain (red envelope) is determined for an

1224   average Al/Si ratio of sediments of 0.23 as sequestration in the floodplain leads to an increase

1225   in the average Al/Si ratio. For carbonates the Si normalized ratios were determined by

1226   averaging all available data for each considered river as carbonate content does not show any

1227   relation to Al/Si. Gomti River sediments as potential analogue for floodplain material are also

1228   shown for comparison. Details on the calculation can be found in Appendix B.

1229

1230
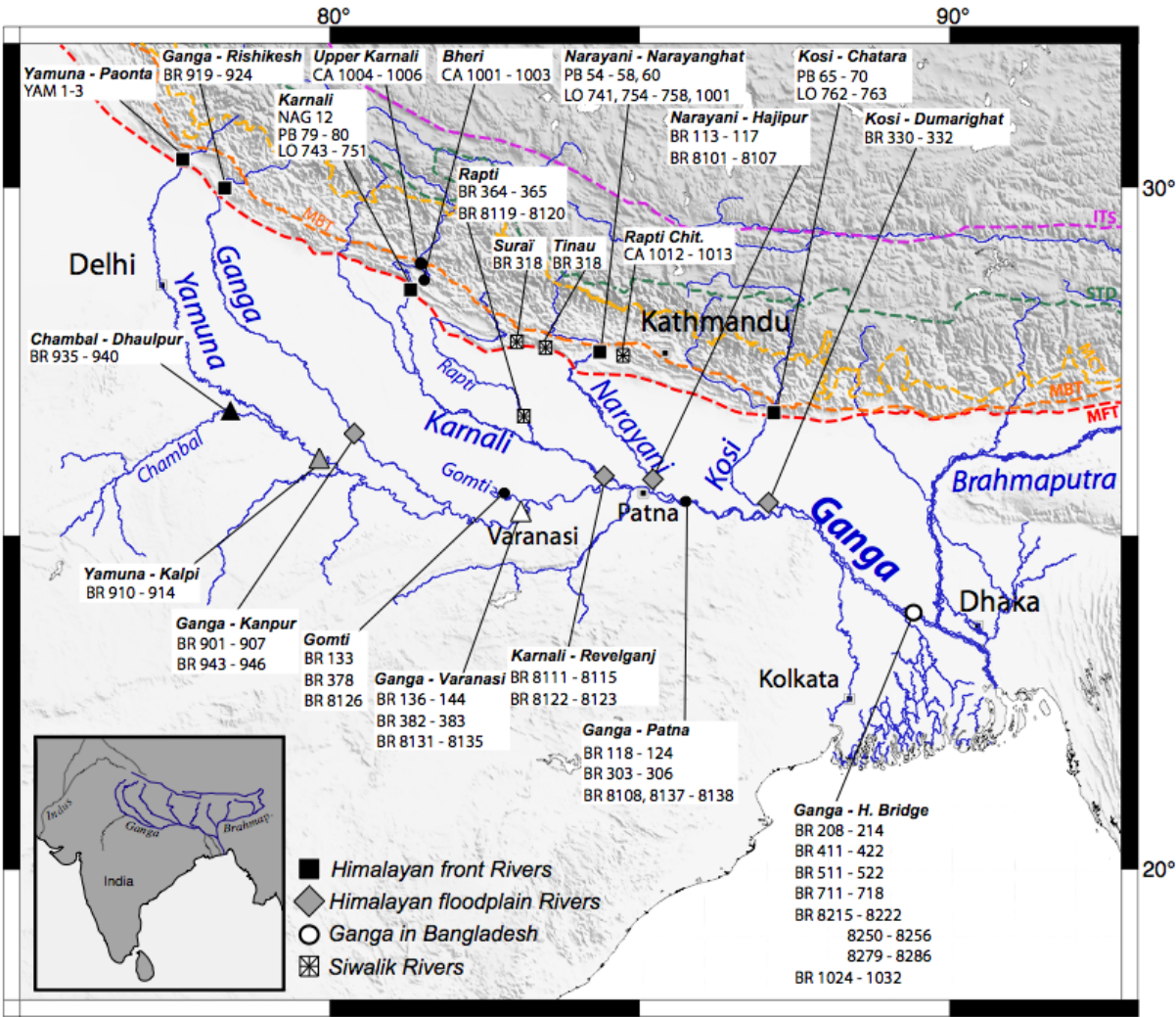
1231 **Figure 1:**

1232

1233

1234   **Figure 2:**
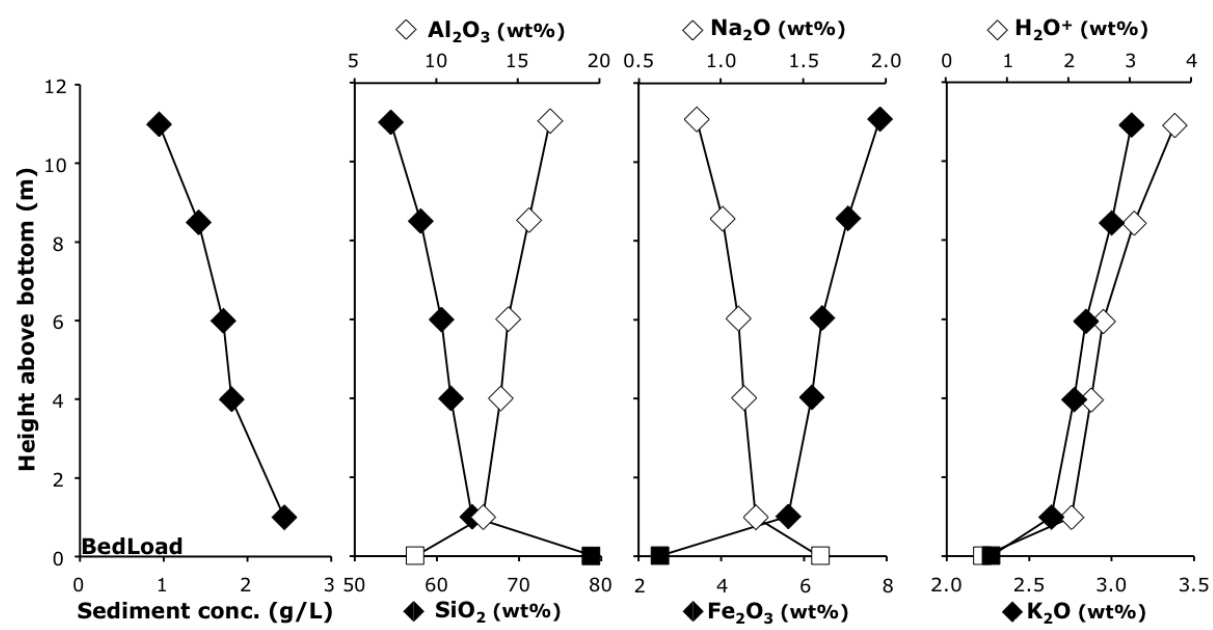
1235

1236

1237   **Figure 3:**
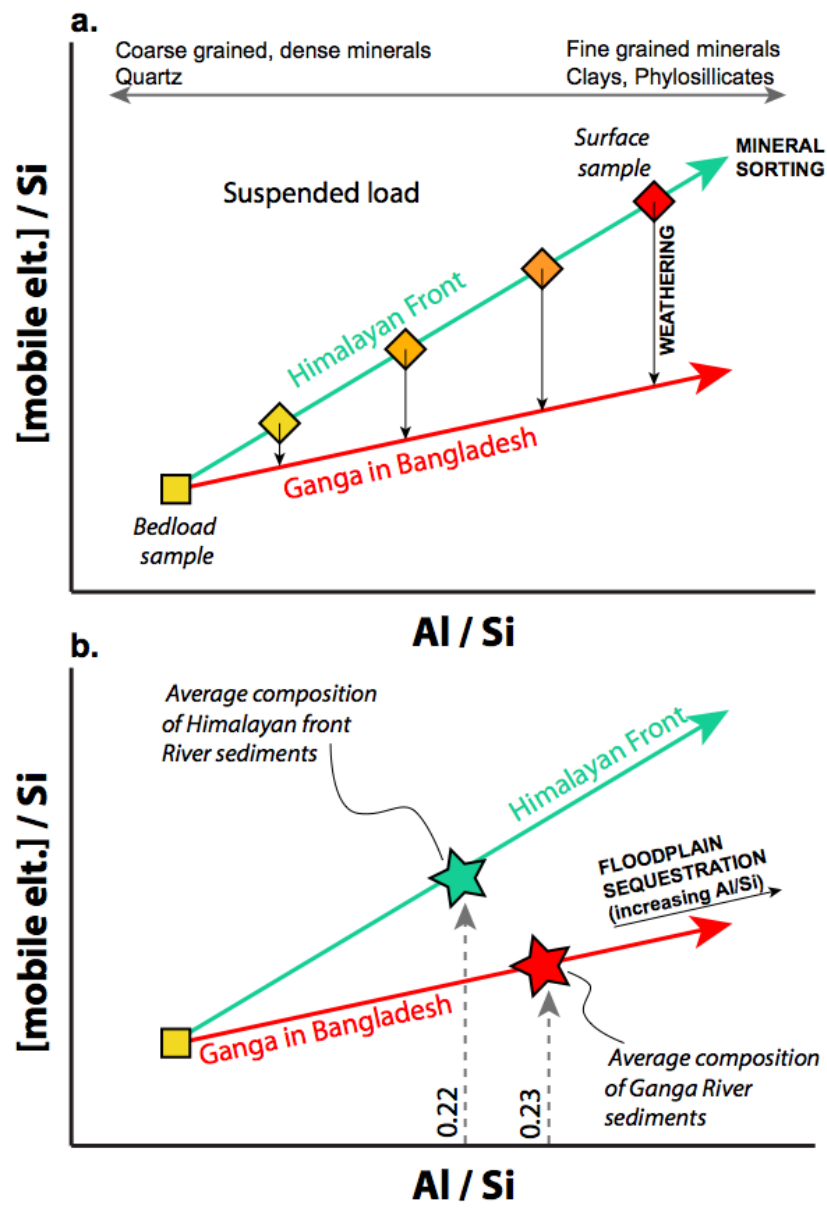
1238

1239   **Figure 4:**
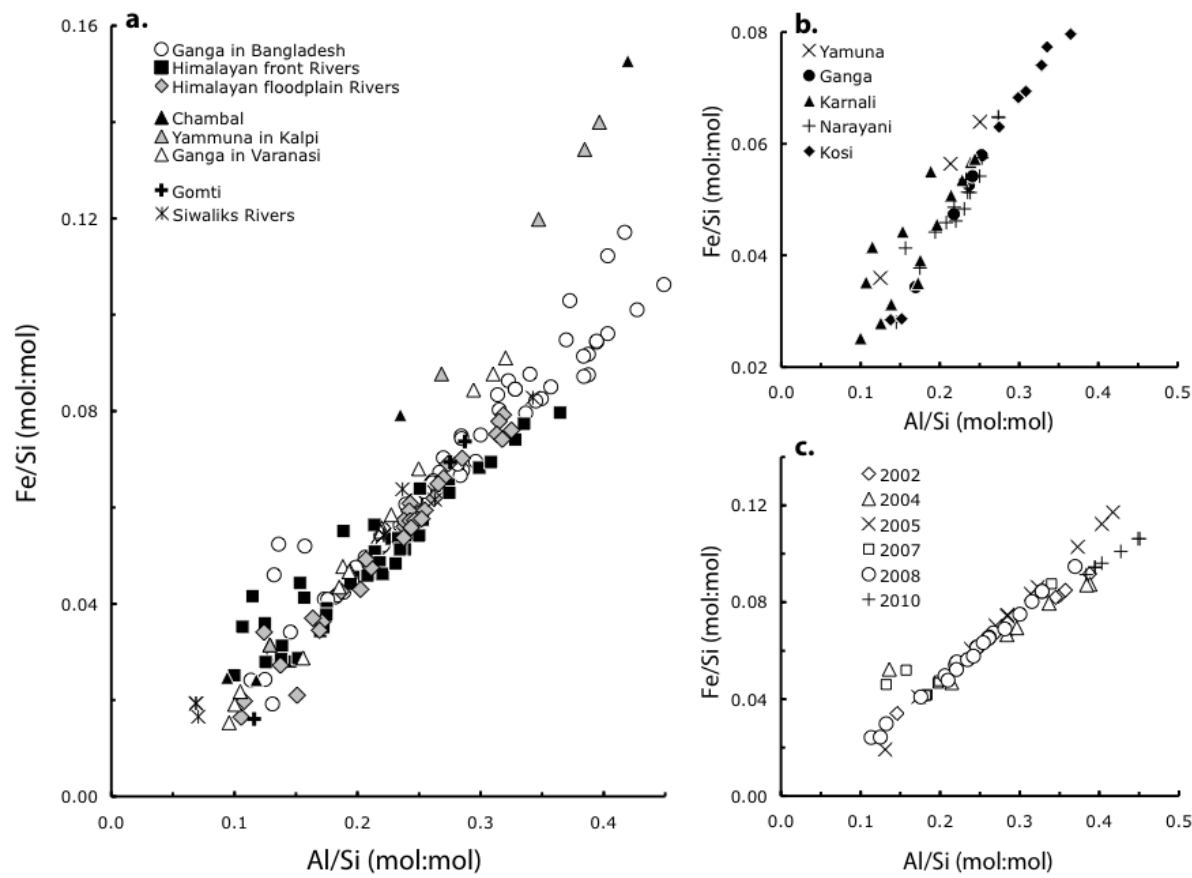
1240

1241
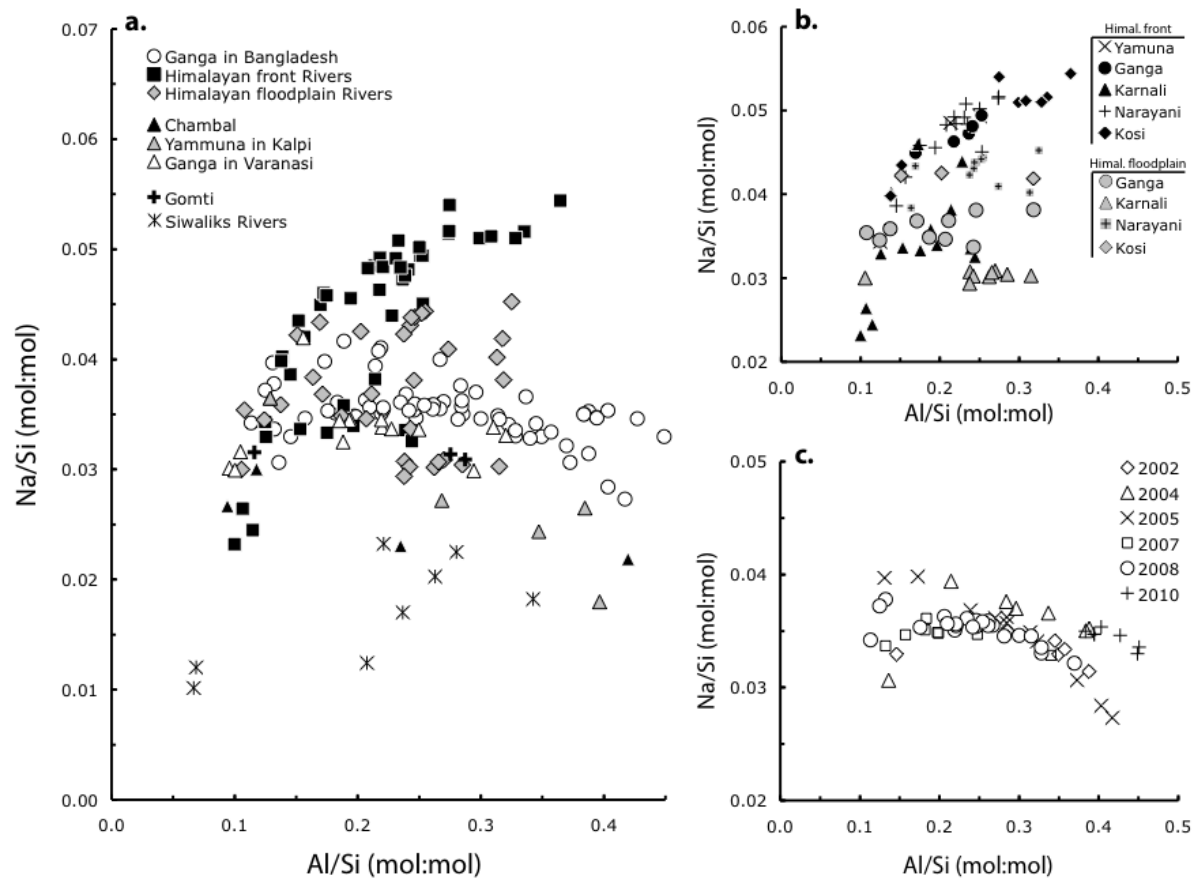
Figure 5:

Figure 6:

Figure 7:

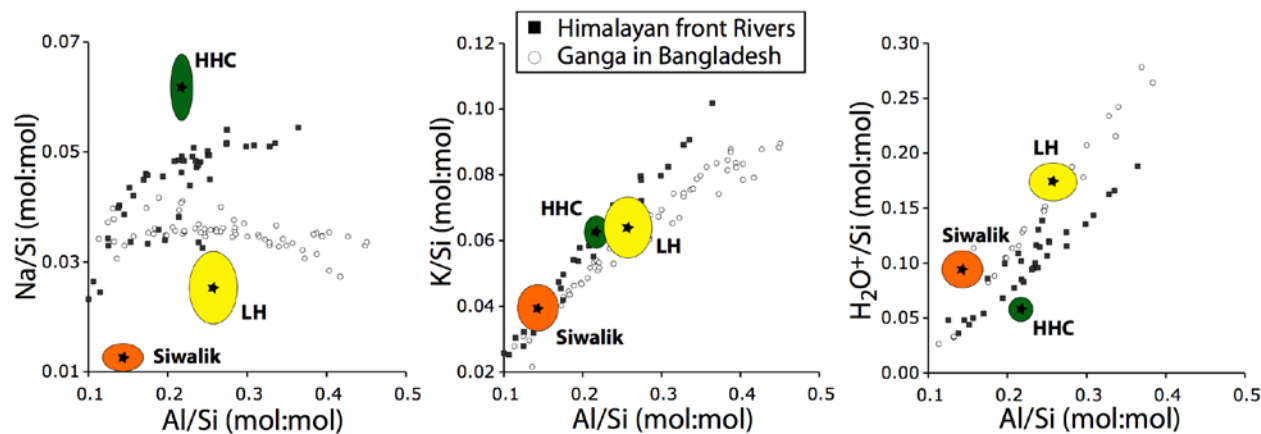**Figure 8:**
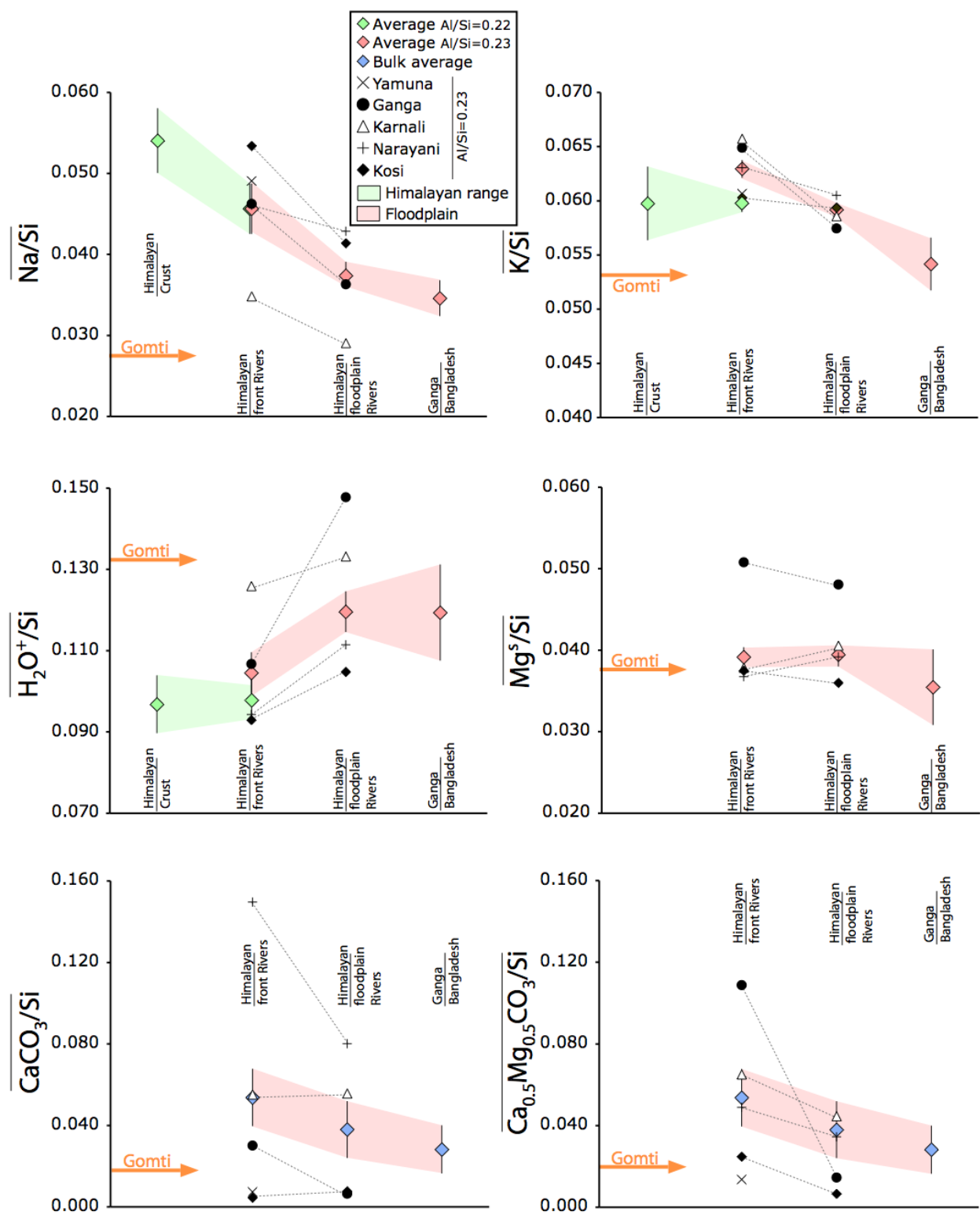
Figure 9:

Figure 10:

1256   **Figure 11:**
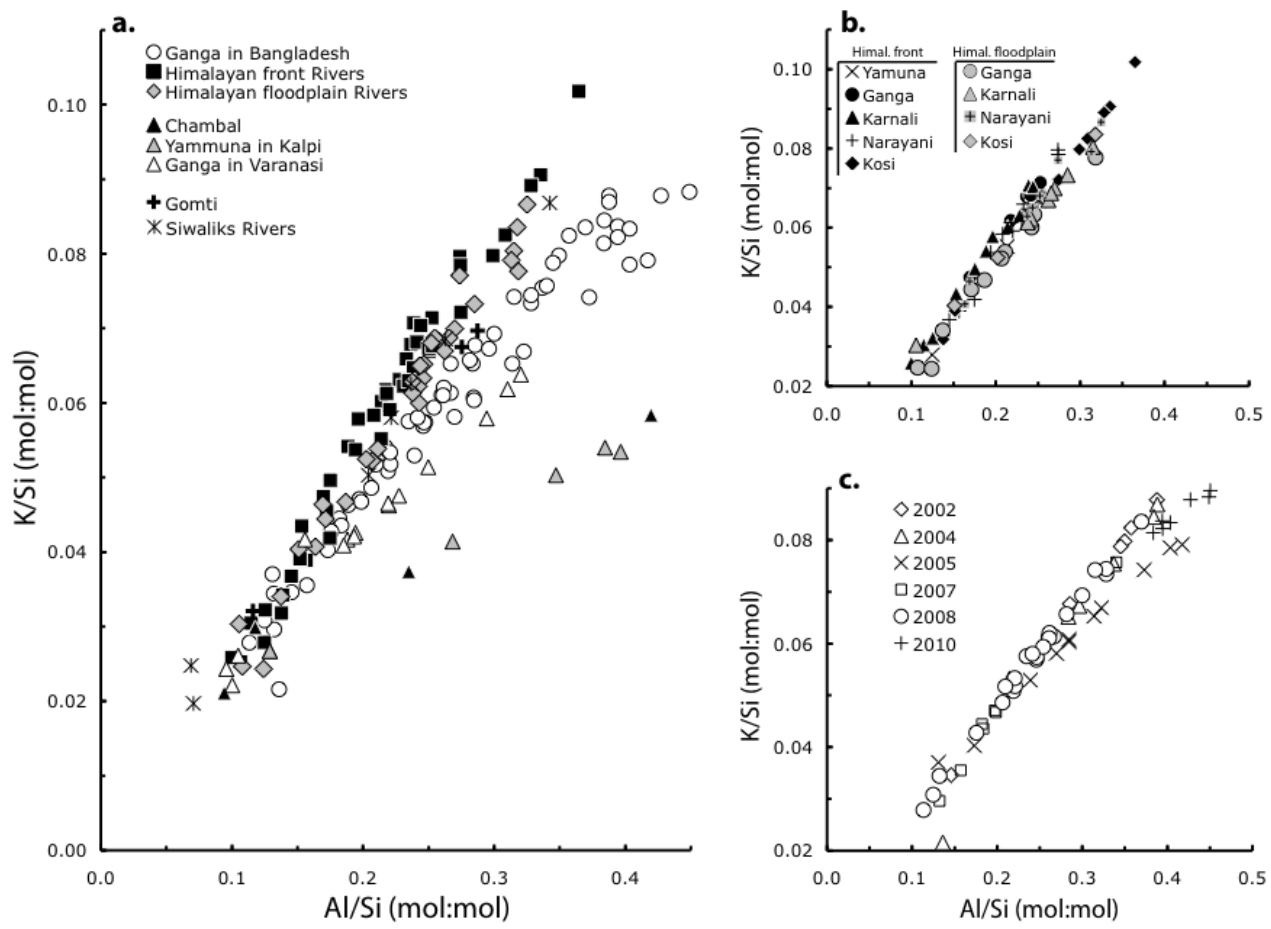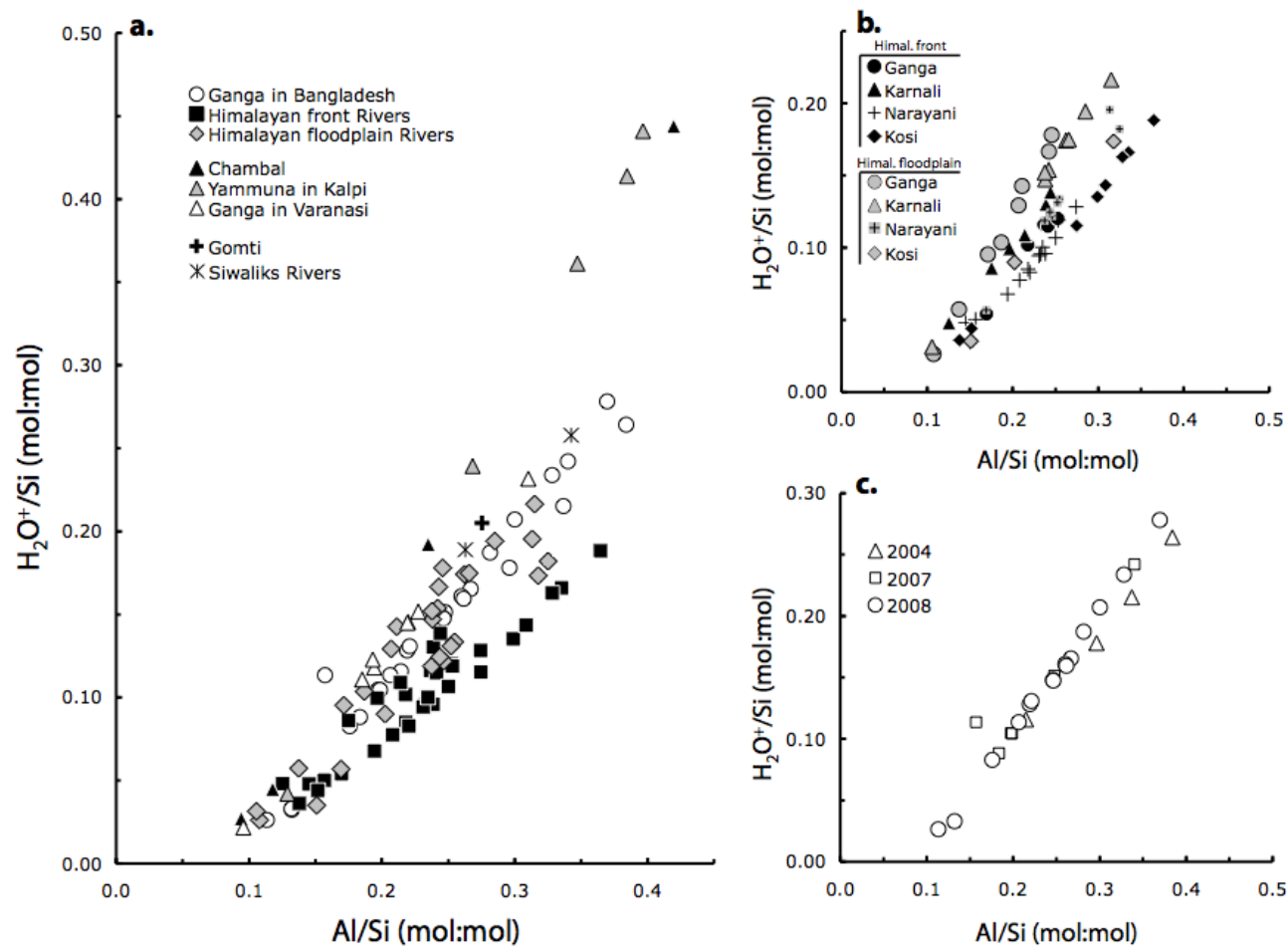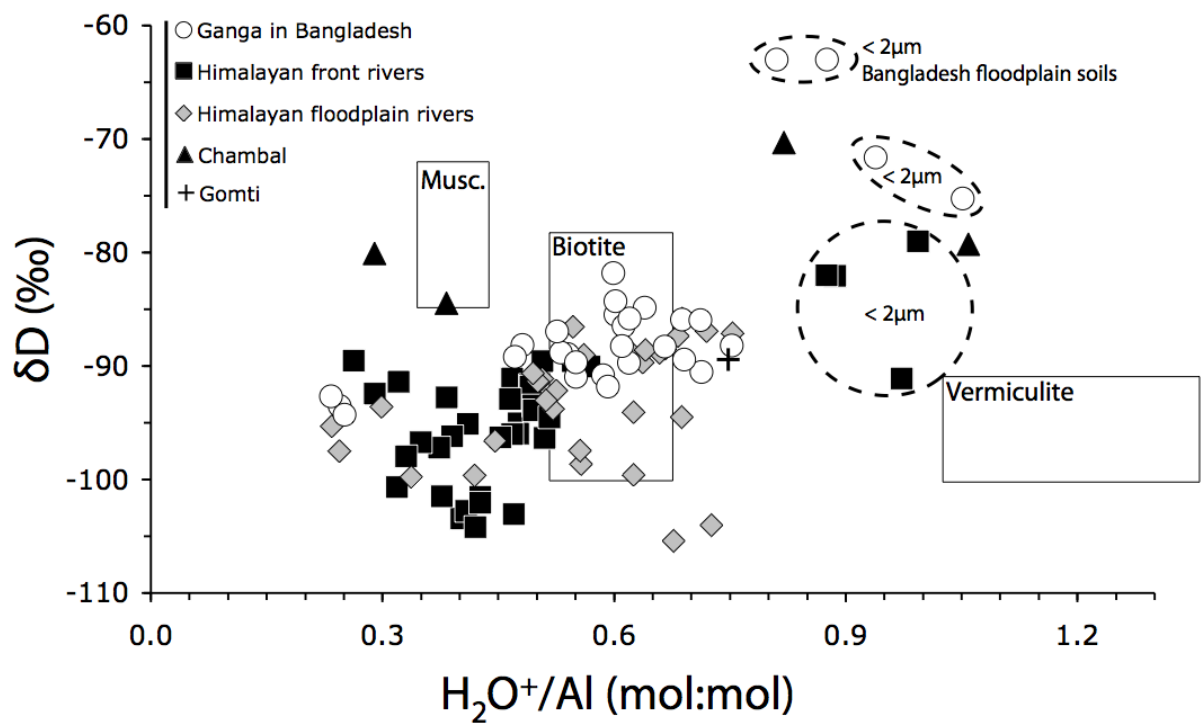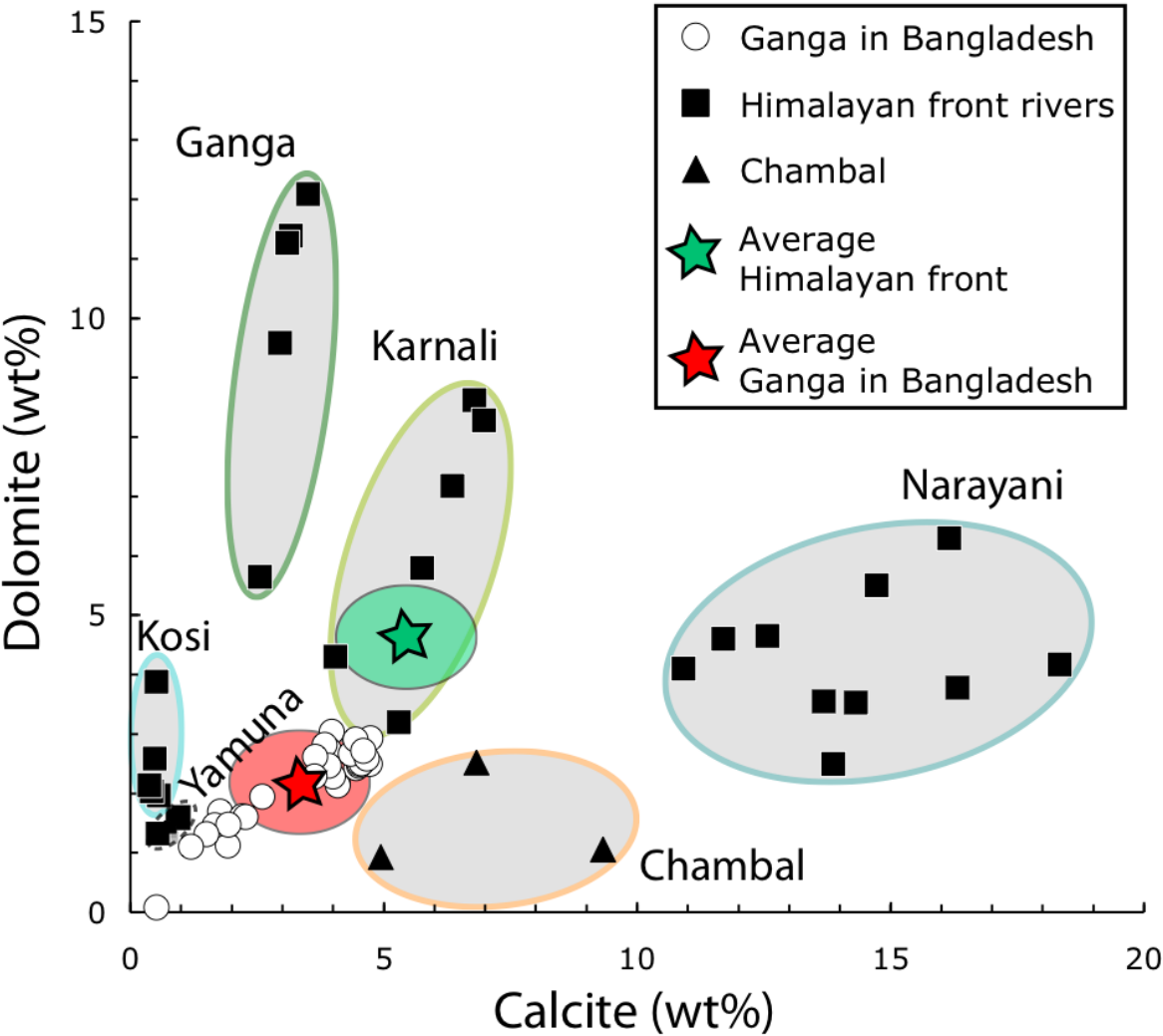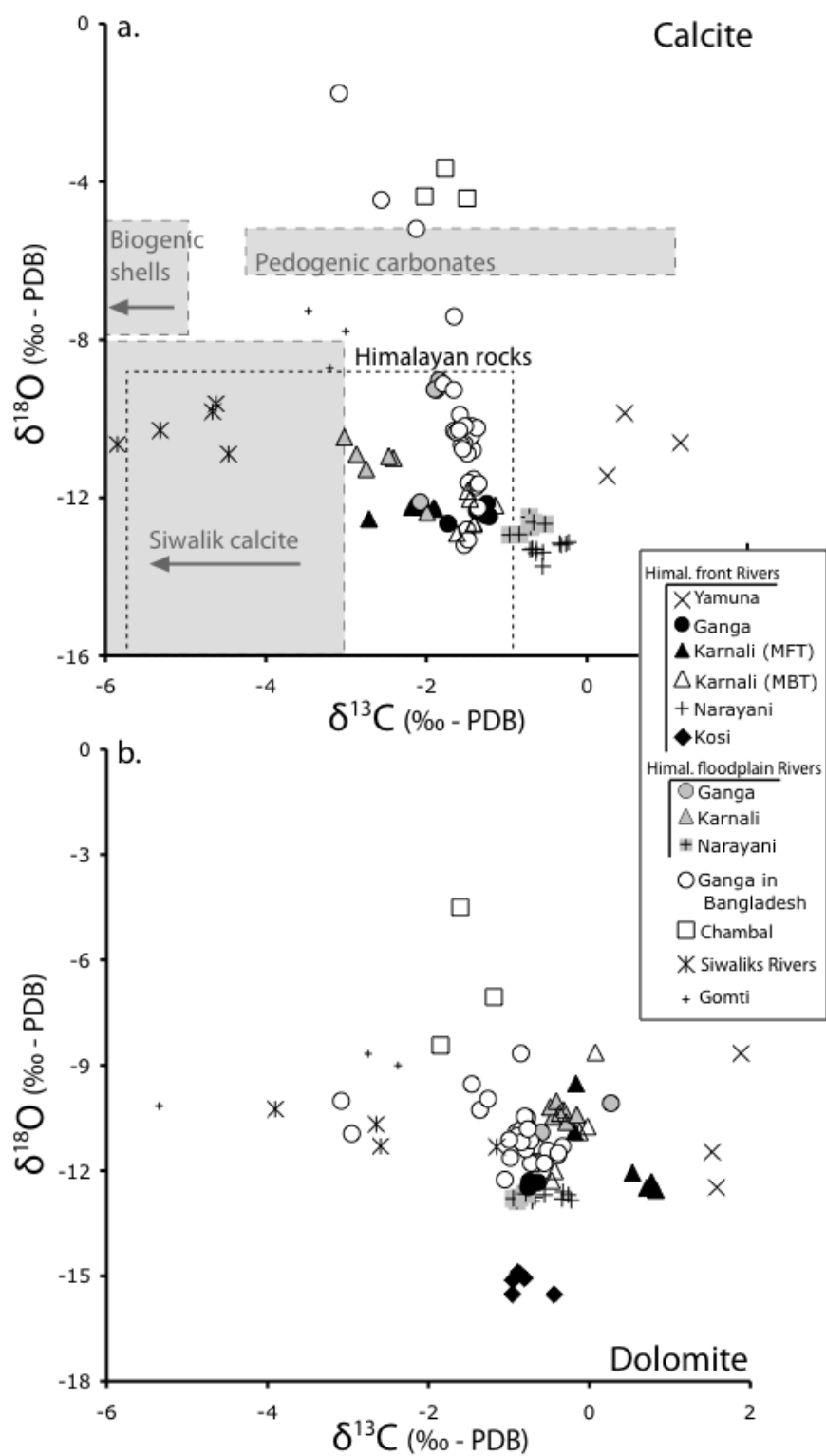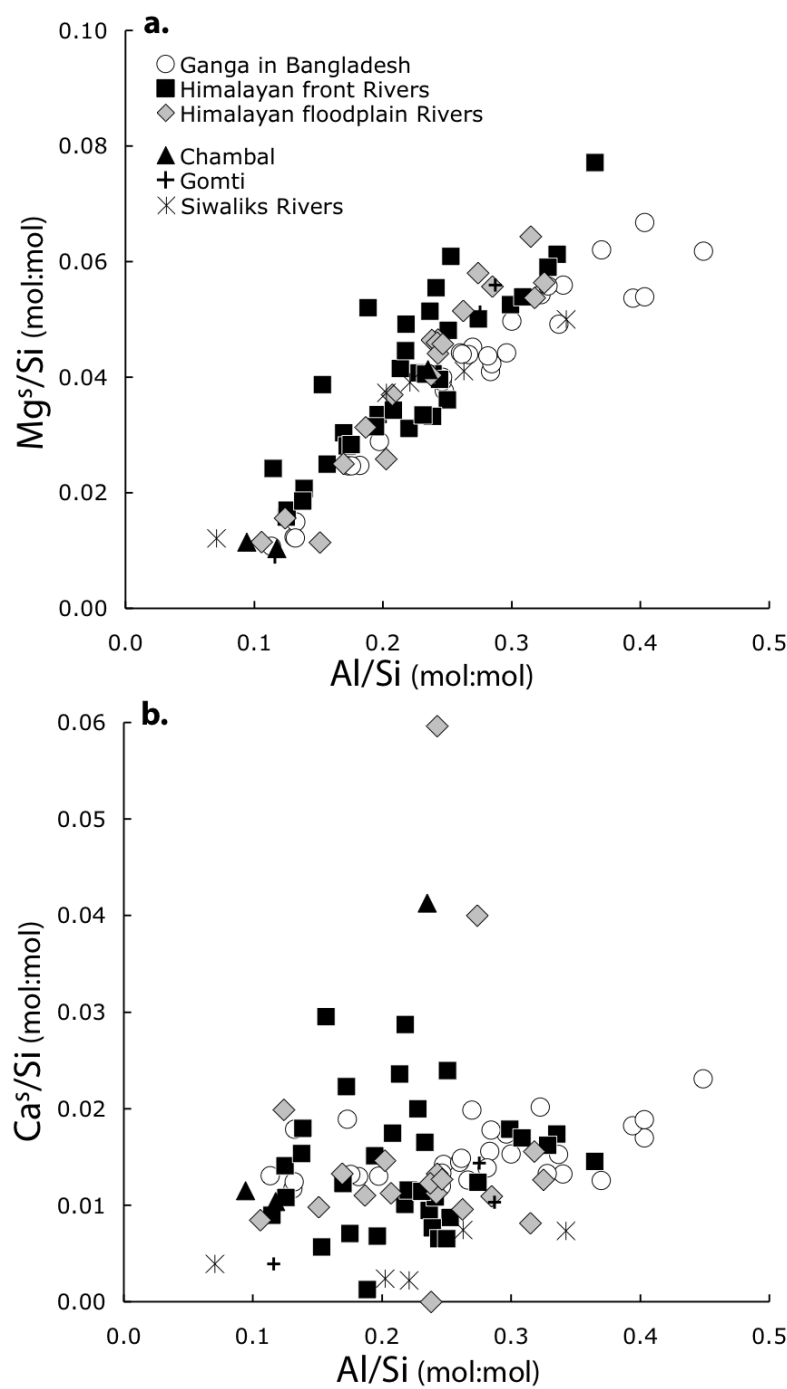
1258   **Figure 12:**

1259

Figure 13:

1262 **Tables:**

1263

1264 **Table 1:** Major elements distribution in the water column and main mineralogical species

1265 contributing to the different elements in the Ganga basin. Mineralogical data based on

1266 analysis mineral separates from Ganga sediments (Garzanti et al., 2011).

1267

1268 **Table 2:** $\Delta \overline{X/_{Si}}$ as computed from equation (2) showing the depletion in mobile elements

1269 relative to silicon for the different compartments of the Ganga basin. Negative values denote

1270 gain of mobile elements.

1271

1272 **Table 3:** Weathering flux generated in the Ganga floodplain as computed from the river

1273 sediments according to equation (4). [1]Sediment derived weathering fluxes are compared to the

1274 dissolved load of the Ganga in Bangladesh (corrected for cyclic contributions) estimated by

1275 Galy and France-Lanord (1999).

1276

1277 **Table 1:**

	Si	Al	Fe	Na	K	Ca	Mg	H_2O^+
Enrichment in water column	bottom	surface	surface	bottom	surface	n.d.	surface	surface
Carrying mineral	Quartz Feldspar Mica	Mica Feldspar Clay	Biotite Clay Fe-hydrox. Opaques	Albite Other feldspar	Mica K-feldspar	Calcite Dolomite Plagioclase	Mica Dolomite	Mica Clay Fe-hydrox.

1278

1279

1280

Table 2:

	Himalayan Range	Floodplain N	Floodplain S	Total floodplain
ΔNa/Si	0.008 (±0.008)	0.008 (±0.003)	0.003 (±0.003)	0.011 (±0.004)
ΔK/Si	0.000 (±0.008)	0.004 (±0.001)	0.005 (±0.003)	0.009 (±0.003)
ΔH$_2$O$^+$/Si	0.000 (±0.016)	-0.015 (±0.007)	0.000 (±0.013)	-0.015 (±0.013)
ΔMg^s/Si	-	0.000 (±0.002)	0.004 (±0.005)	0.004 (±0.005)
ΔCaCO$_3$/Si	-	0.015 (±0.020)	0.010 (±0.018)	0.025 (±0.018)
Δ(Ca,Mg)CO$_3$/Si	-	0.024 (±0.009)	0.004 (±0.010)	0.029 (±0.009)

1282

1283

1284 **Table 3:**

	10^9 mol/yr	% of total dissolved load[1]
φ **Na**	53 (±18)	70 %
φ **K**	42 (±13)	140 %
φ **H$_2$O$^+$**	-71 (±62)	-
φ **Silicate Mg**	17 (±23)	-
φ **Carbonate Mg**	69 (±22)	-
φ **Total Mg**	86 (±32)	100 %
φ **Silicate Ca**	*< 10*	-
φ **Carbonate Ca**	189 (±92)	-
φ **Total Ca**	199 (±100)	98 %

1285